XFELO cavity. Where we are?

Yuri Shvyd'ko

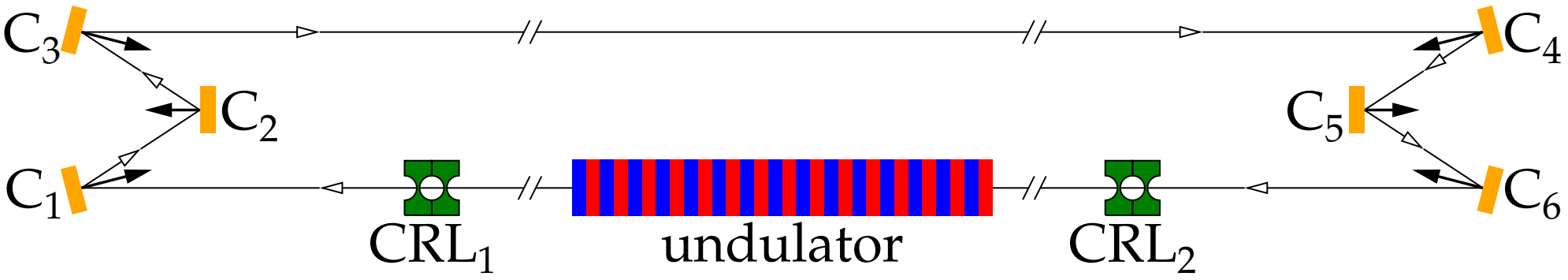

Acknowledgments

XFELO collaboration (2009-now)

Kwang-Je Kim (APS)
Deming Shu (APS)
Stanislav Stoupin (APS)
Ryan Lindberg (APS)
Tomasz Kolodziej (APS)
Vladimir Blank (TISNCM)
Sergey Terentev (TISNCM)

Acknowledgments

XFELO collaboration (2009-now)

Kwang-Je Kim (APS)
Deming Shu (APS)
Stanislav Stoupin (APS)
Ryan Lindberg (APS)
Tomasz Kolodziej (APS)
Vladimir Blank (TISNCM)
Sergey Terentev (TISNCM)

Thanks to:

Bill Fawley, (LBNL)
Sven Reiche (SLS)
Sergey Polyakov (TISNCM)
Stan Whitcomb (LIGO)
Harald Sinn (European-XFEL)
Tim Roberts (APS)
Kurt Goetze (APS)
Ayman Said (APS)
Thomas Gog (APS)
T. J. Maxwell (SLAC)
J. Arthur (SLAC)
Y. Ding (SLAC)
J. Frisch (SLAC)
J. Hastings (SLAC)
Z. Huang (SLAC)
J. Krzywinski (SLAC)
G. Marcus (SLAC)

Acknowledgments

XFELO collaboration (2009-now)

Kwang-Je Kim (APS)
Deming Shu (APS)
Stanislav Stoupin (APS)
Ryan Lindberg (APS)
Tomasz Kolodziej (APS)
Vladimir Blank (TISNCM)
Sergey Terentev (TISNCM)

Many thanks to Makina Yabashi for valuable input & discussions

Thanks to:

Bill Fawley, (LBNL)
Sven Reiche (SLS)
Sergey Polyakov (TISNCM)
Stan Whitcomb (LIGO)
Harald Sinn (European-XFEL)
Tim Roberts (APS)
Kurt Goetze (APS)
Ayman Said (APS)
Thomas Gog (APS)
T. J. Maxwell (SLAC)
J. Arthur (SLAC)
Y. Ding (SLAC)
J. Frisch (SLAC)
J. Hastings (SLAC)
Z. Huang (SLAC)
J. Krzywinski (SLAC)
G. Marcus (SLAC)

Content

- X-ray cavity designs
- X-ray cavity feasibility studies
- Conclusions and Outlook

XFEL Oscillator Scheme & Prerequisites

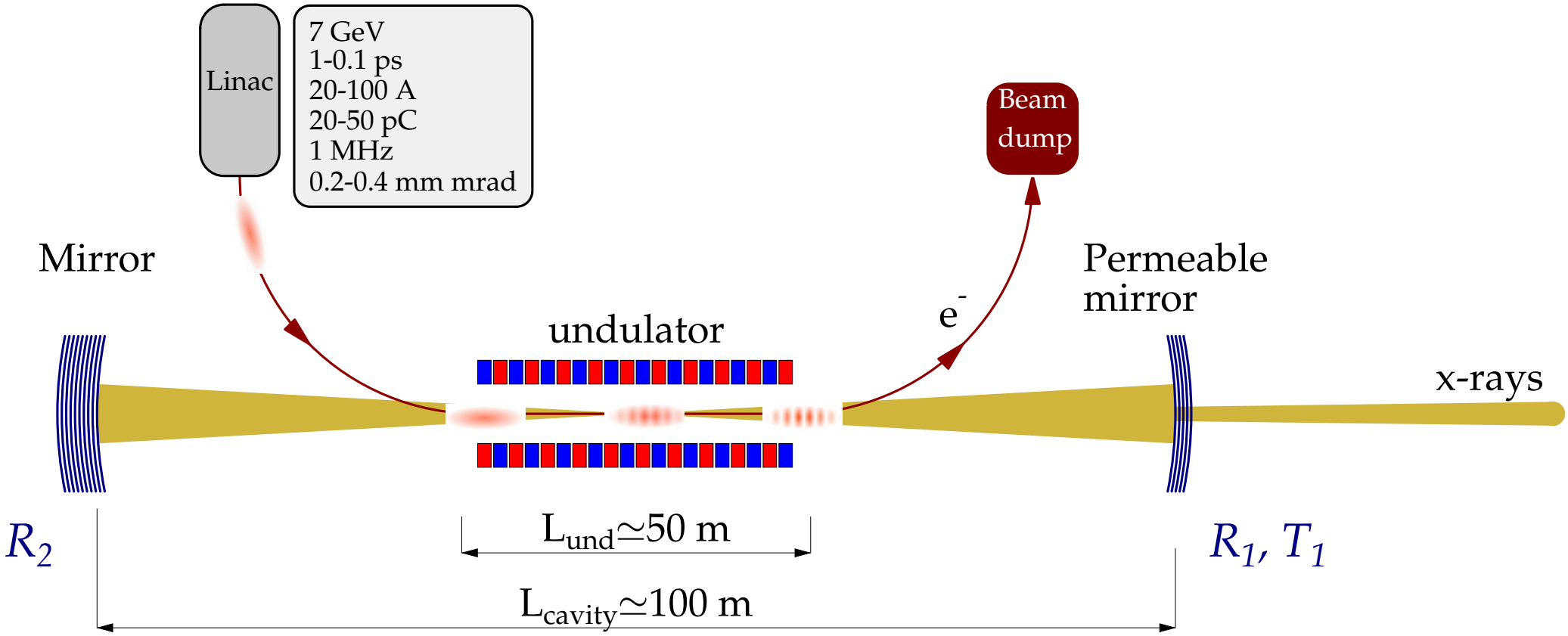

XFELO is a low gain machine.

K.-J. Kim, Yu. Shvyd'ko, S. Reicher, PRL 100 (2008) 244802.

XFEL Oscillator Scheme & Prerequisites

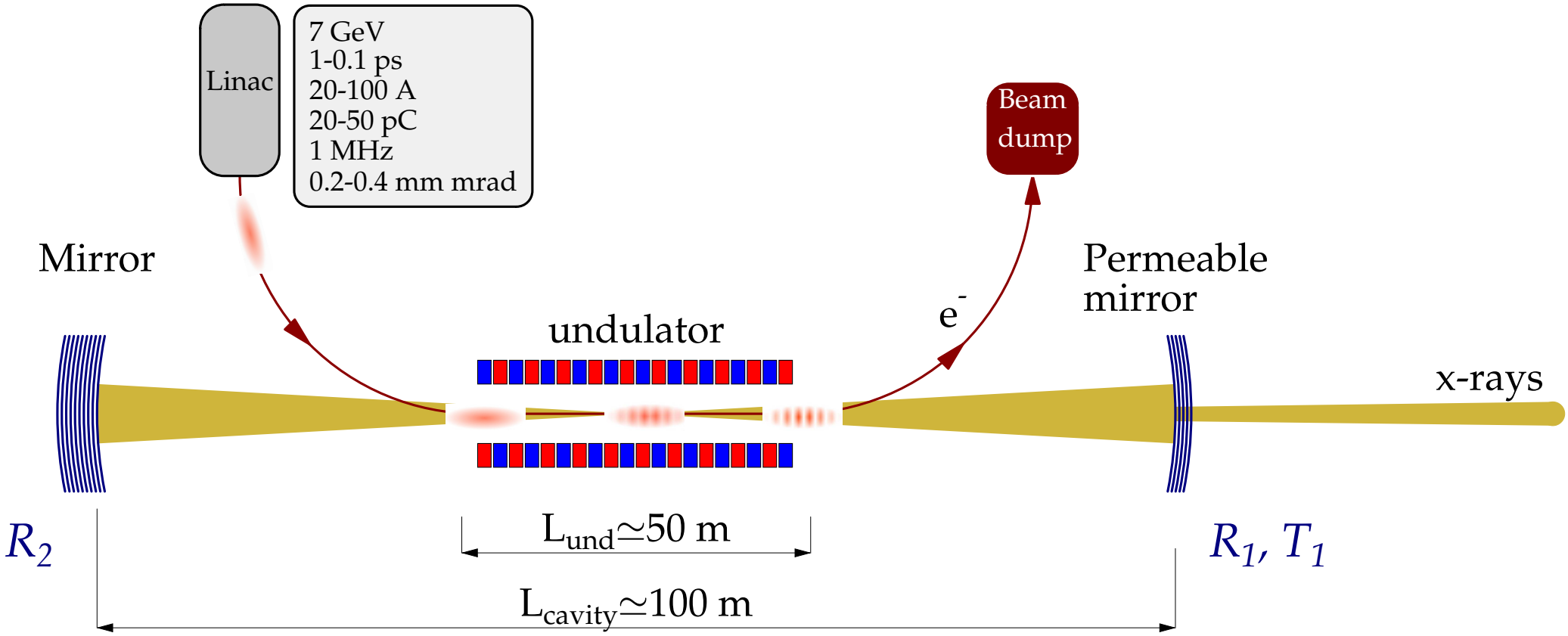

XFELO is a low gain machine. **It requires:**

- **ultra-low-emittance ($\varepsilon_n \simeq 0.2 - 0.4$ mm mrad) electron beams,**
- **low-loss x-ray crystal cavity (losses $\lesssim 15\%$)** $R_1, R_2 \gtrsim 95\%$, $T_1 \simeq 4\%$

K.-J. Kim, Yu. Shvyd'ko, S. Reicher, PRL 100 (2008) 244802.

Two-Crystal Cavity

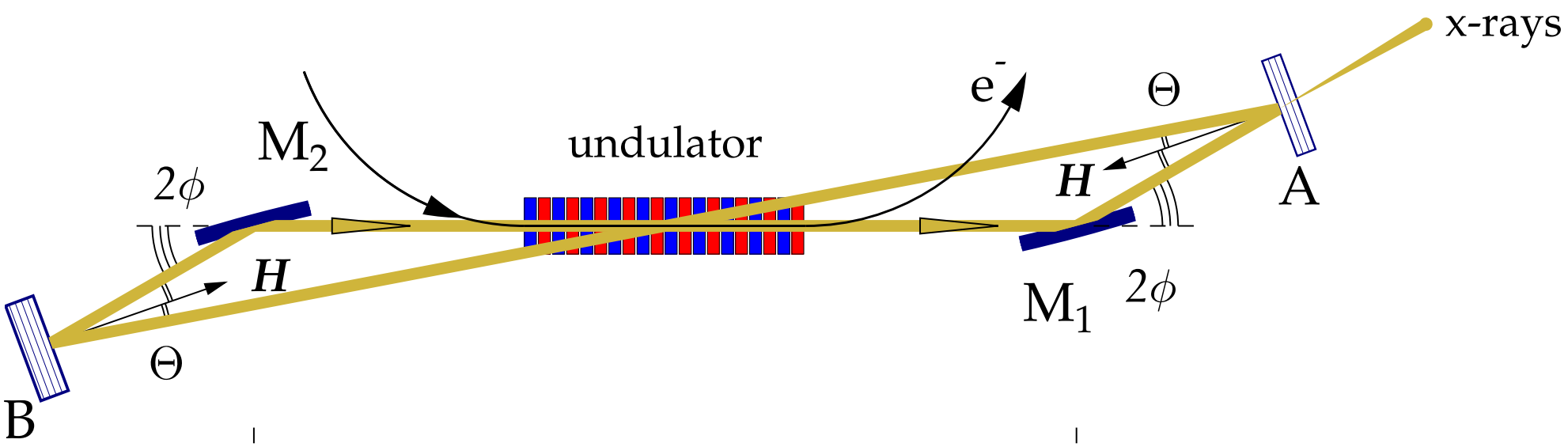

$$R_A \times R_B \times R_{M_1} \times R_{M_2} \simeq 0.9 \qquad T_A \simeq 0.04$$

Two-Crystal Cavity - Non-Tunable

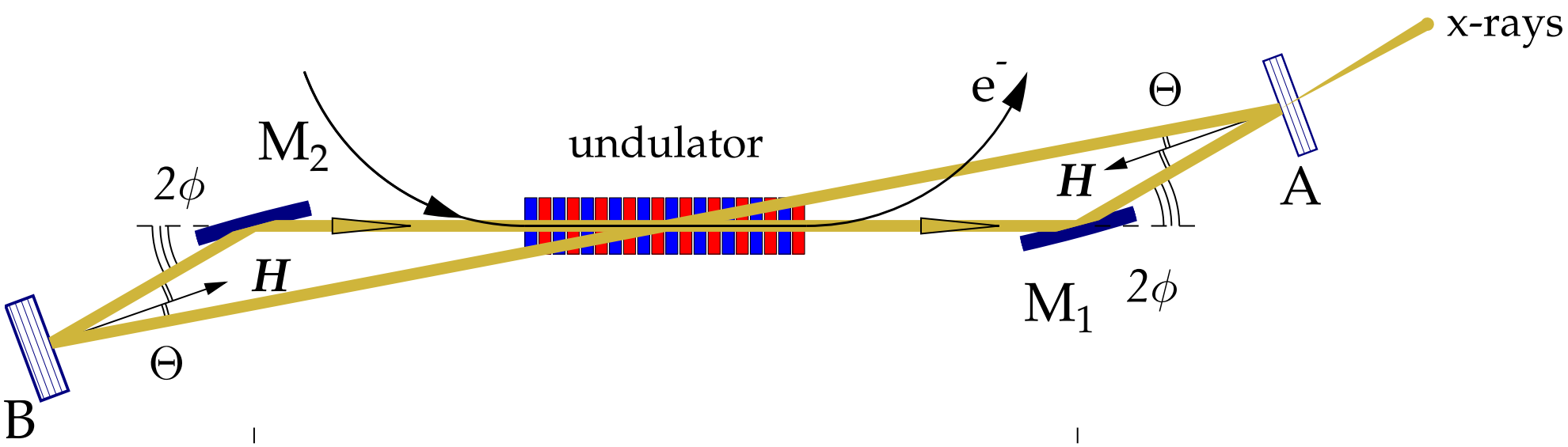

$$R_A \times R_B \times R_{M_1} \times R_{M_2} \simeq 0.9 \qquad T_A \simeq 0.04$$

$E = E_H \cos\Theta \quad \Rightarrow \quad$ **Two-crystal scheme is not tunable.**

Because, it is necessary to keep small $\phi \lesssim 2$ mrad

and therefore small $\Theta \lesssim 2$ mrad, for high reflectivity of the mirrors.

Tunable Cavity

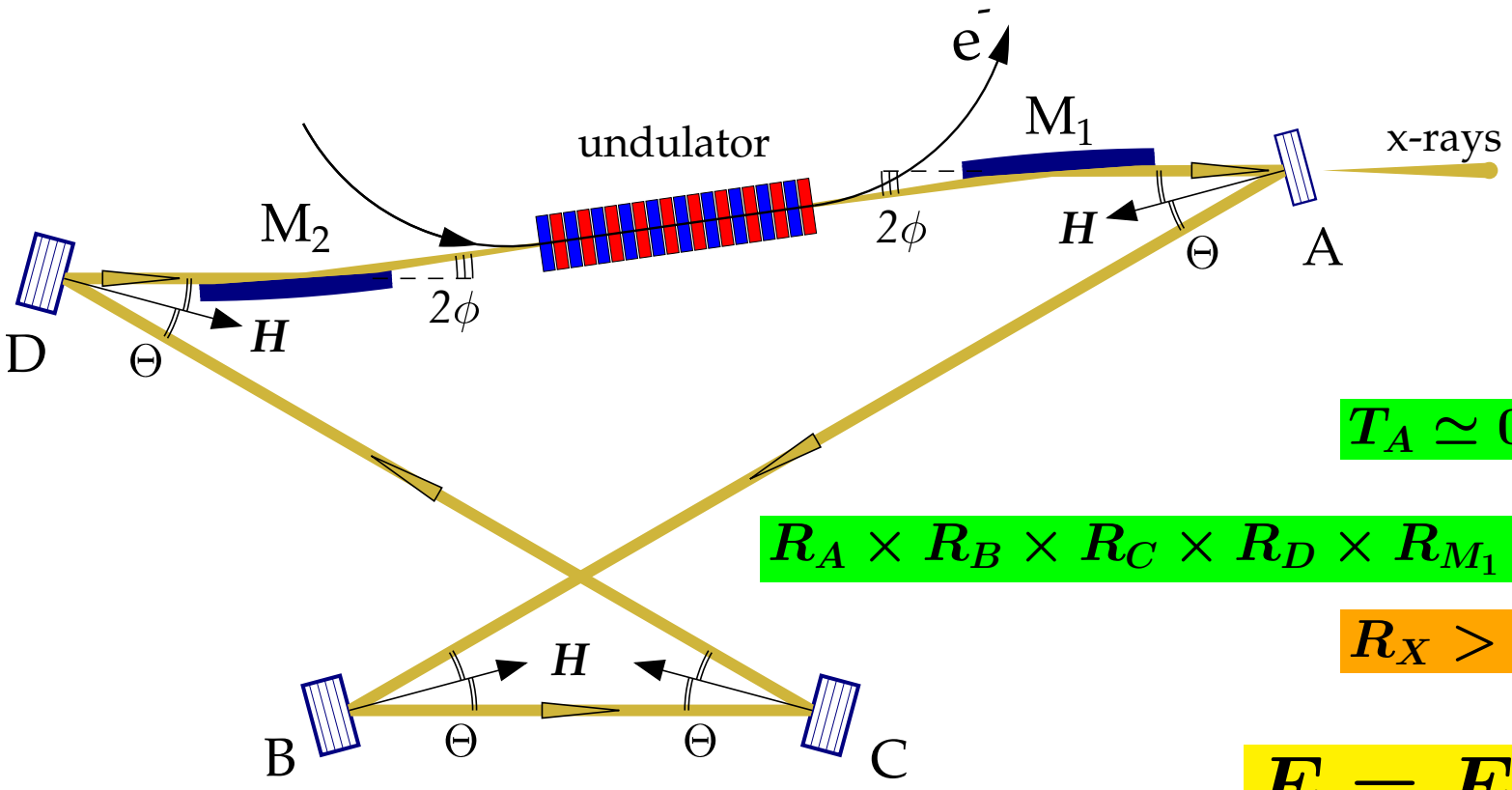

$$T_A \simeq 0.04$$

$$R_A \times R_B \times R_C \times R_D \times R_{M_1} \times R_{M_2} \simeq 0.9$$

$$R_X > 98\%$$

$$E = E_H \cos\Theta$$

A four-crystal (A,B,C, and D) x-ray optical cavity allows photon energy E tuning in a broad range by changing the incidence angle Θ.

R.M.J. Cotterill, Appl. Phys. Lett., 12 (1968) 403

K.-J. Kim, and Yu. Shvyd'ko, Phys. Rev. STAB (2009)

Tunable Cavity with CRLs

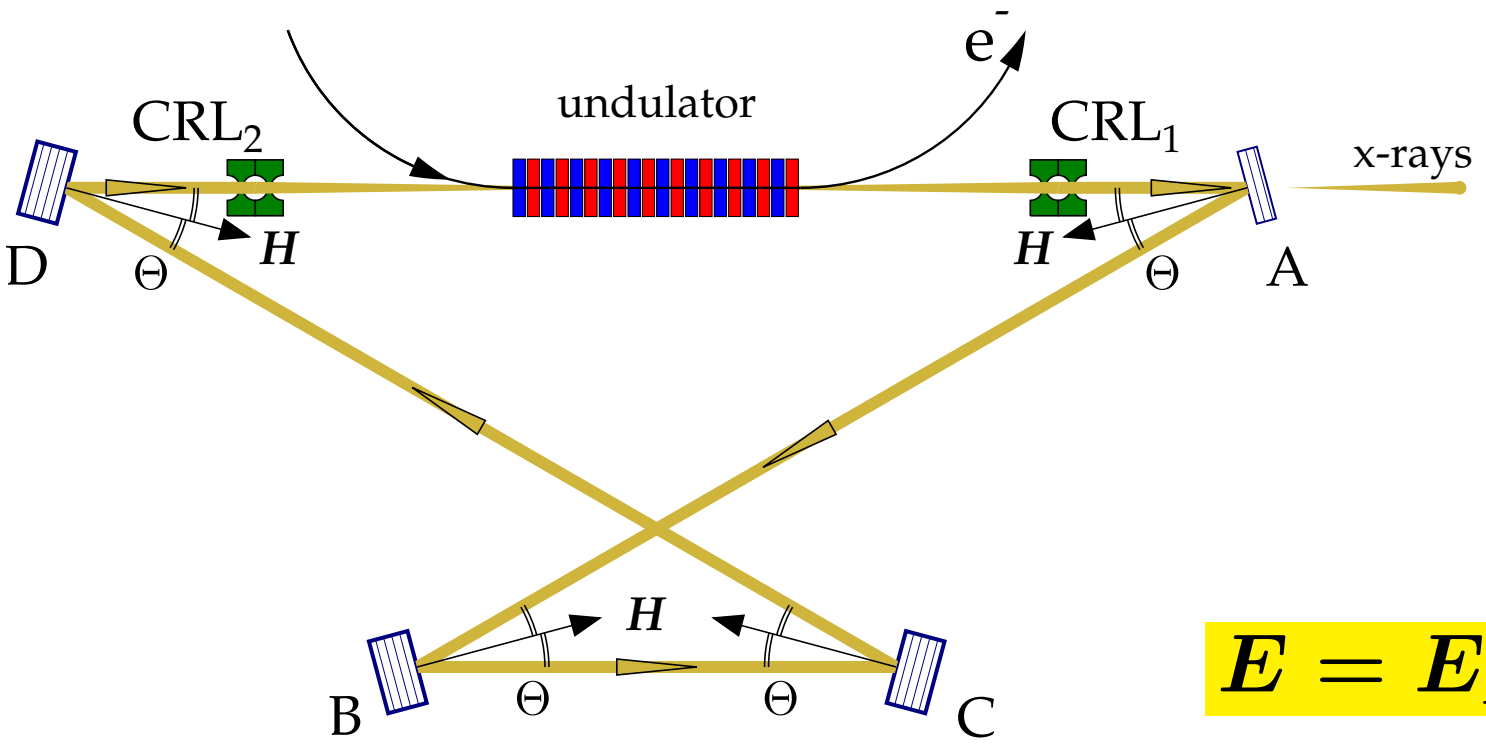

$$E = E_H \cos\Theta$$

A four-crystal (A,B,C, and D) x-ray optical cavity allows photon energy E tuning in a broad range by changing the incidence angle Θ.

K.-J. Kim, and Yu. Shvyd'ko, Phys. Rev. STAB (2009)

XFELO Tunability

XFELO with zigzag cavity in ESA building @ SLAC

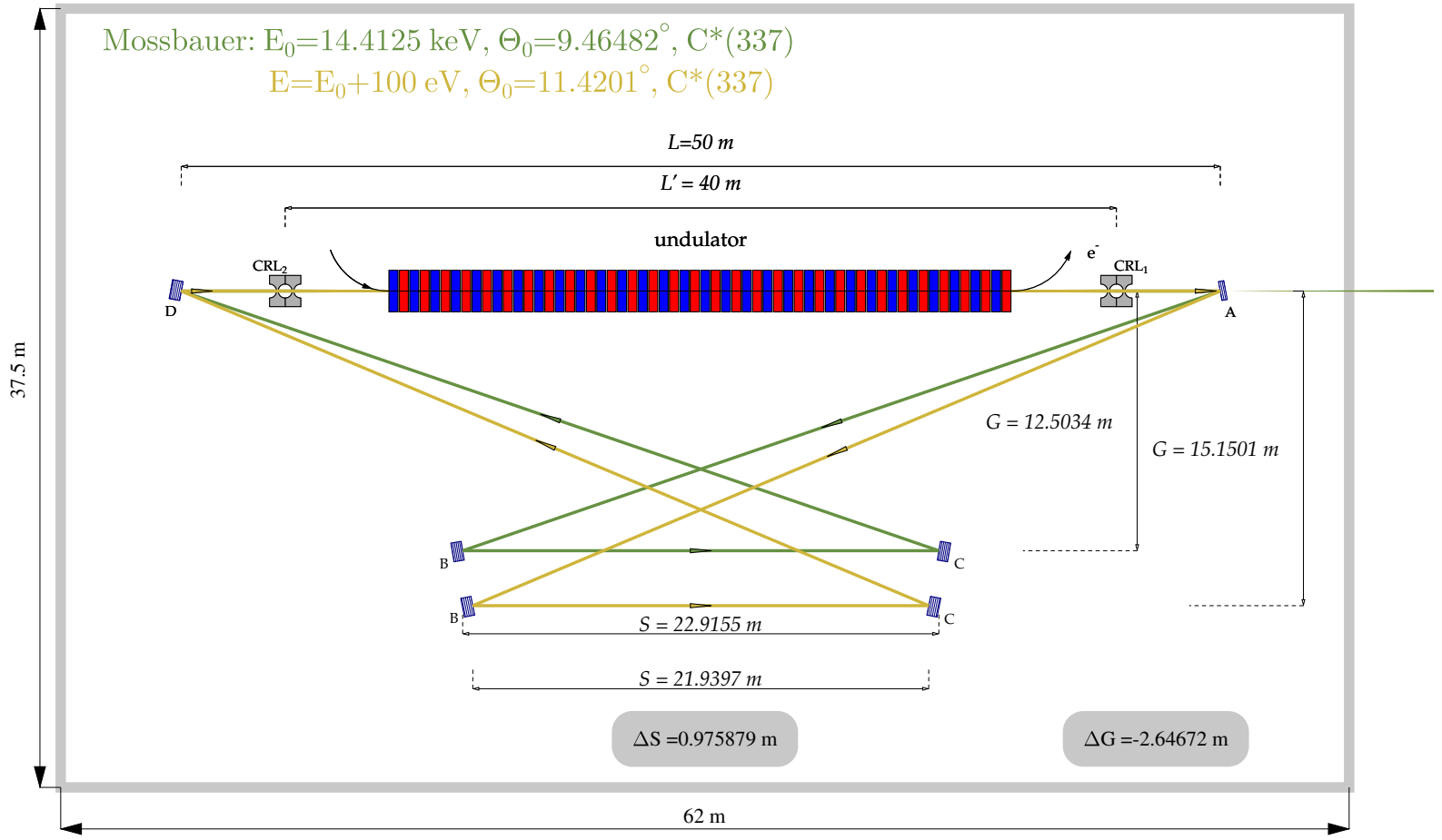

$\simeq \pm 100$ eV tuning range is feasible.

Tunable Compact Non-Coplanar Cavity

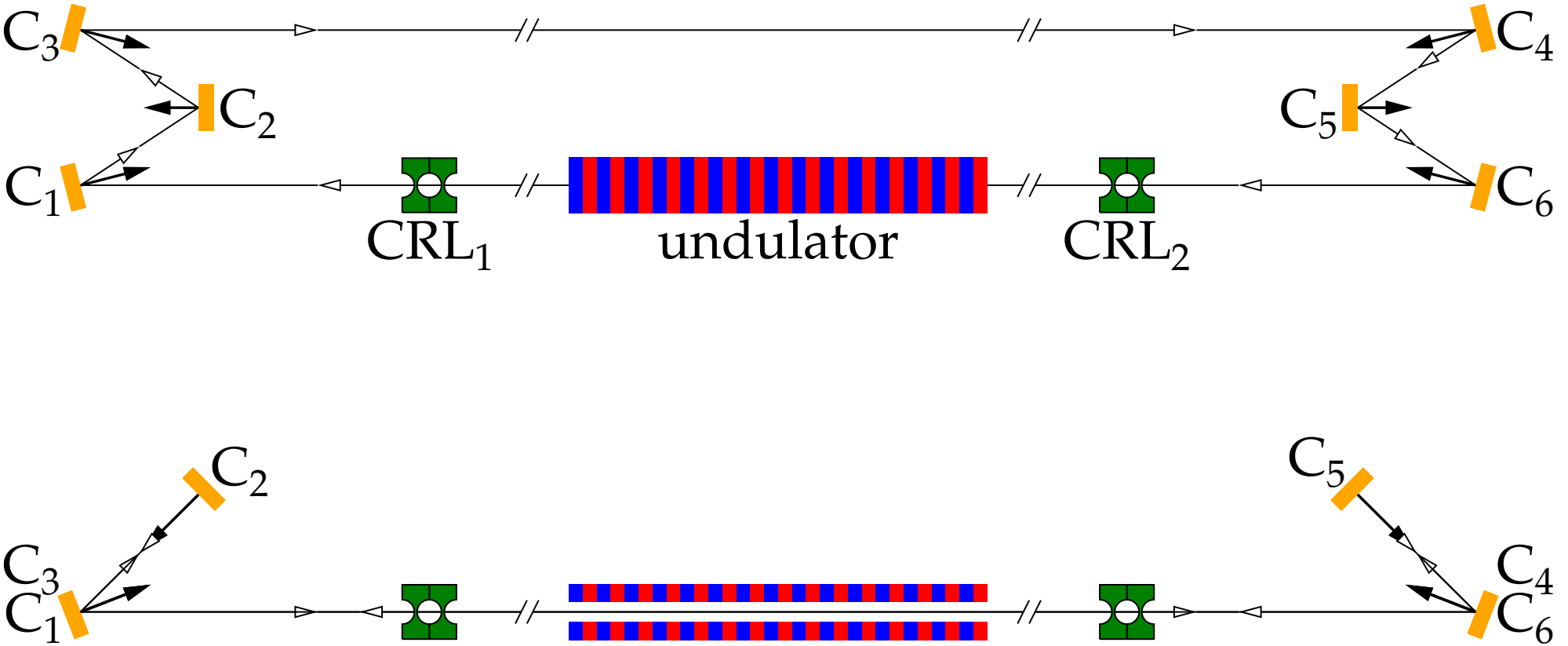

A six-crystal (C_1, C_2, ... C_6) x-ray optical cavity allows photon energy E tuning in a broad range by changing the incidence angle Θ.

Tunable Compact Non-Coplanar Cavity

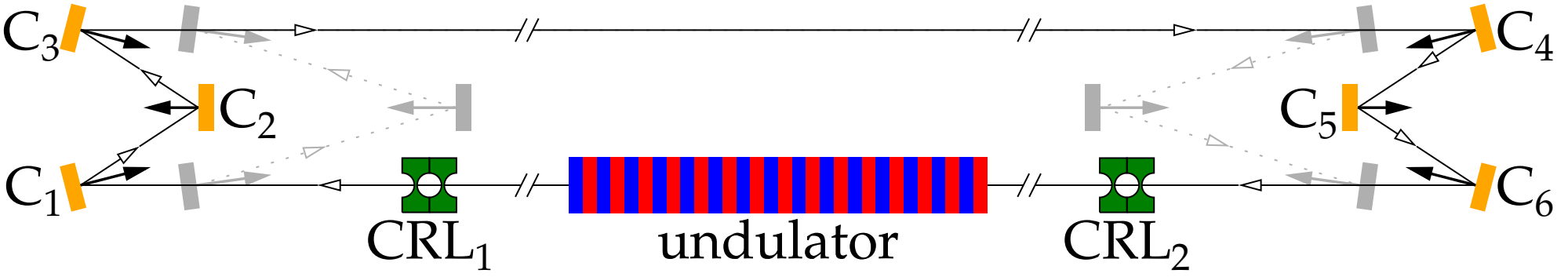

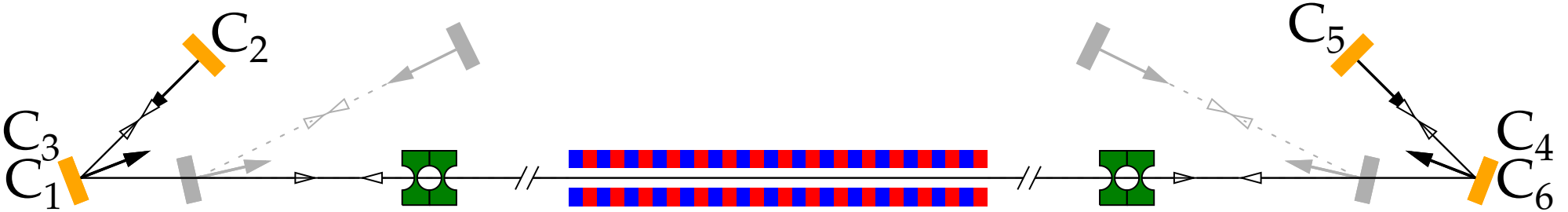

A six-crystal (C_1, C_2, ... C_6) x-ray optical cavity allows photon energy E tuning in a broad range by changing the incidence angle Θ.

Can be tuned easily by $\Delta E \simeq 1$ keV $E \simeq 14$ keV

Yu. Shvyd'ko, Beam Dynamics Newsletter No. 60, April 2013, 68-83

XFELO Spectral Bandwidth

Determined by the length of the electron bunch.

Fourier-transform-limited after $\gtrsim 200$ passes.

Crystal cavity helps to generate the monochromatic seed.

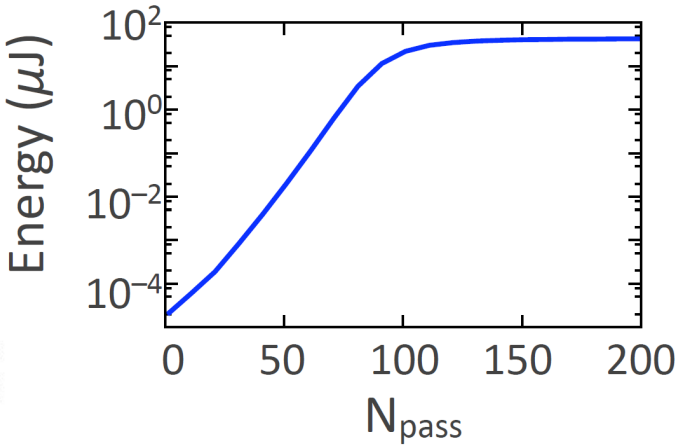

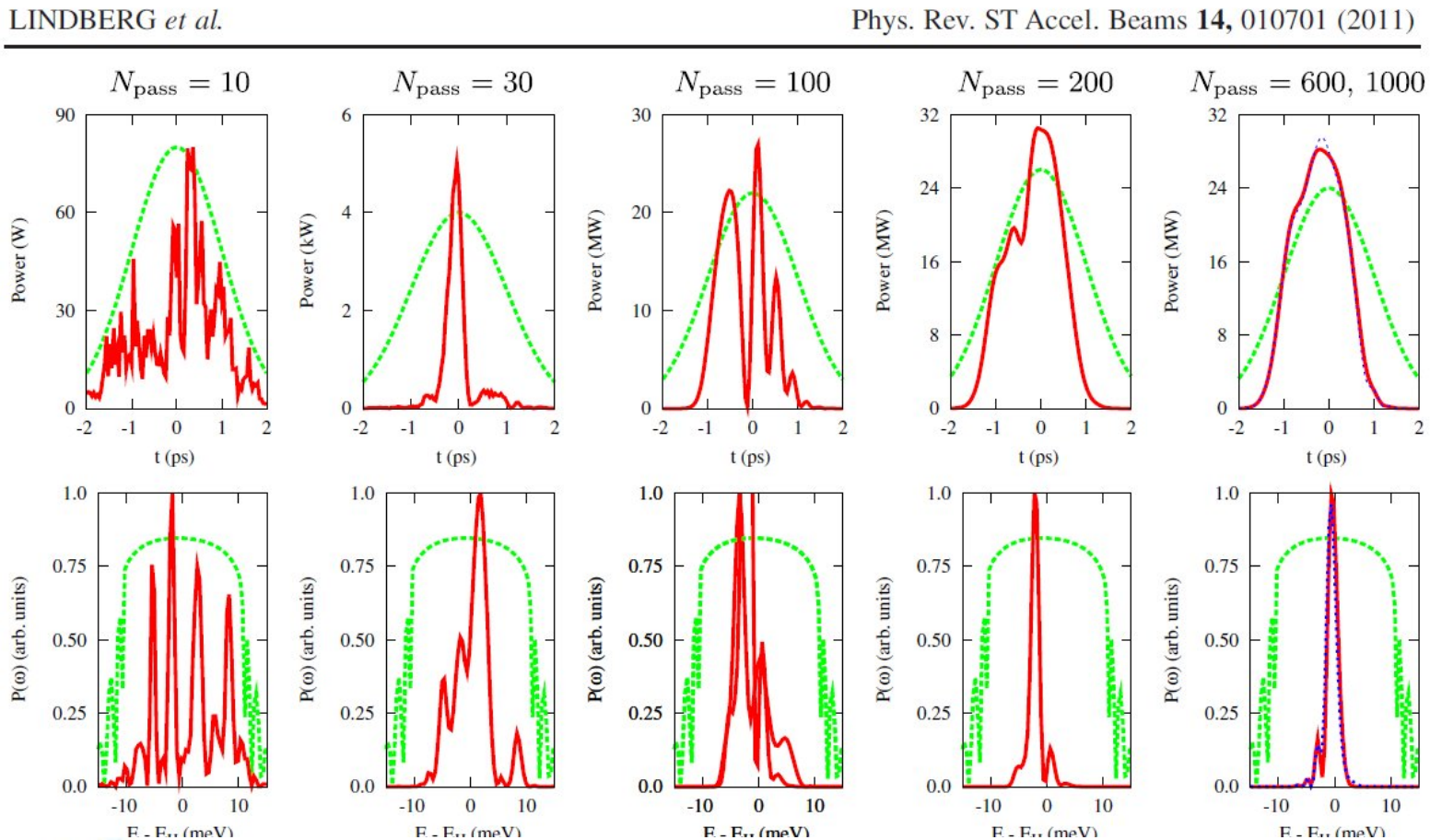

XFELO Cavity Technical Challenges

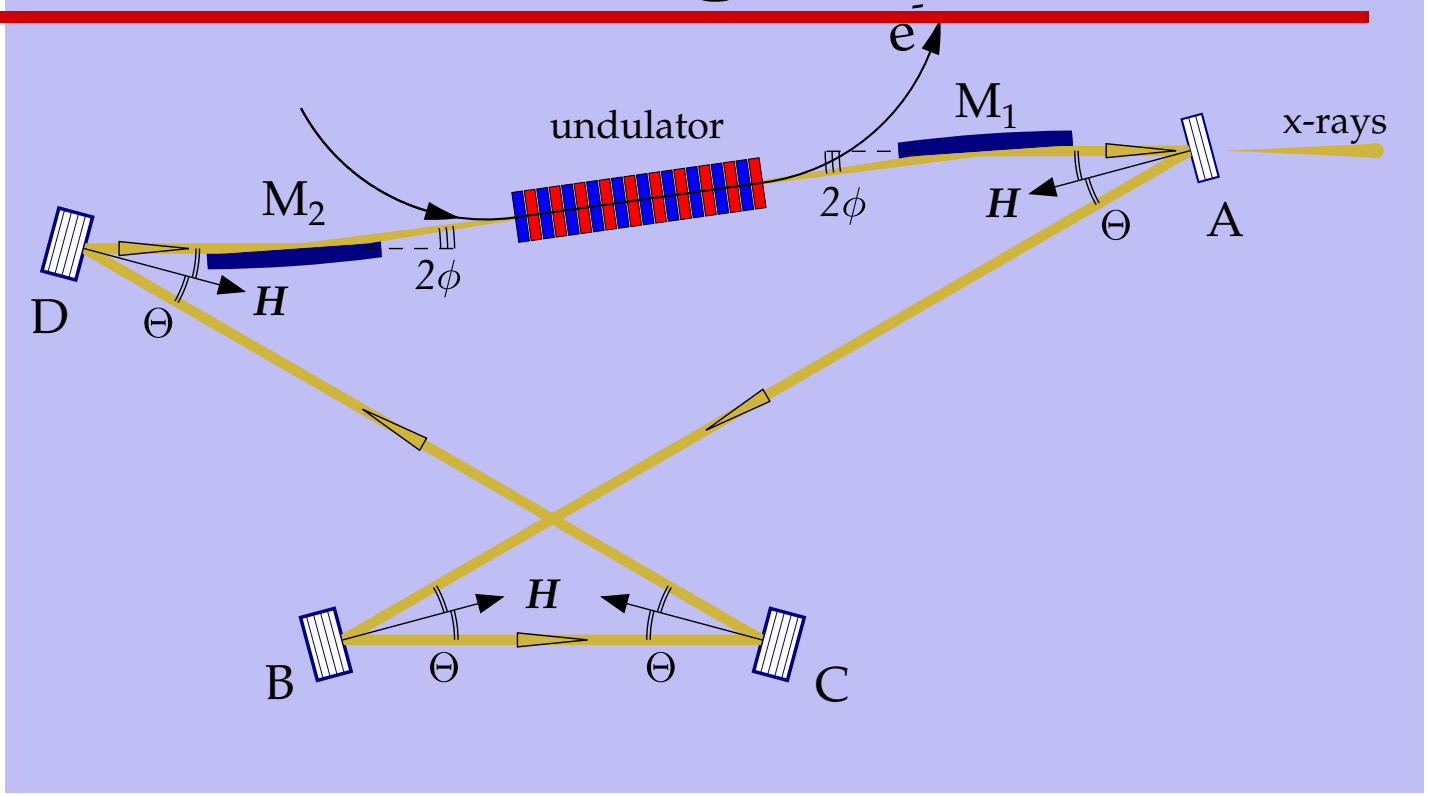

- **Efficient ($> 98\%$) & wavefront preserving focusing/collimating optics**
- **Crystal reflectivity: is the required $> 98\%$ reflectivity in backscattering feasible?**
- **Heat load problem: reflection band instability due to thermal variations $\lesssim 1$ meV.**
- **Angular stability: $\delta\theta \lesssim 10$ nrad (rms)**
  Spatial stability: $\delta L \lesssim 3$ μm (rms) $\rightarrow$ $\delta L/L \lesssim 3 \times 10^{-8}$
- **Radiation resilience to 4 kW/mm^2 irradiation.**

Focusing and Collimating Optics

- **State-of-the-art x-ray ellipsoidal mirrors may feature close to 99% reflectivity & $\lesssim 0.1$ μrad figure error**

Yumoto et al SPring-8

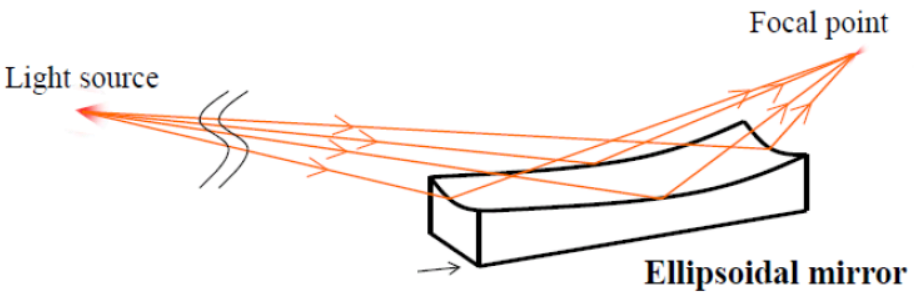

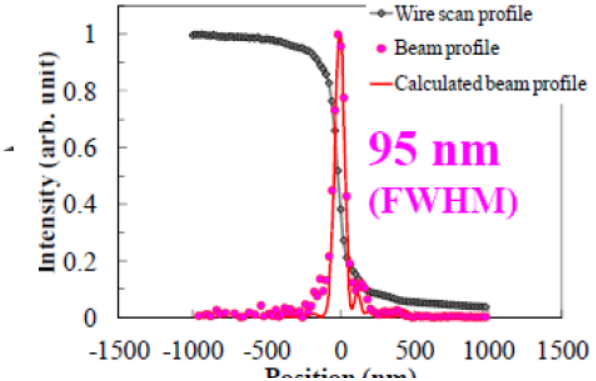

Yumoto-san

- **Paraboloidal Be compound refractive lenses (CRL) may feature high transparency $\simeq$ 99% for large focal length $\gtrsim$ 20 m.**

A. Snigirev et al & B. Lengeler et al ESRF

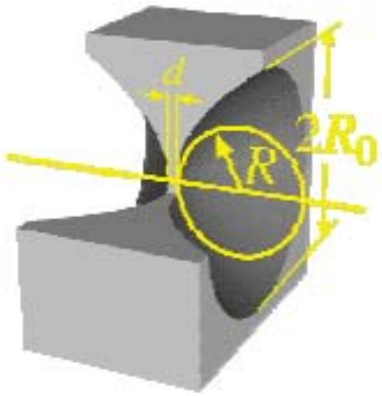

For 14.4 keV, f = 21.1 m, d=30 um σ_r = 28 um,
Crystalline Be, IF 1 grade: *Tr* = 99.74%
PS20 E grade (atten. length 60% of IF-1): *Tr* = 99.56%

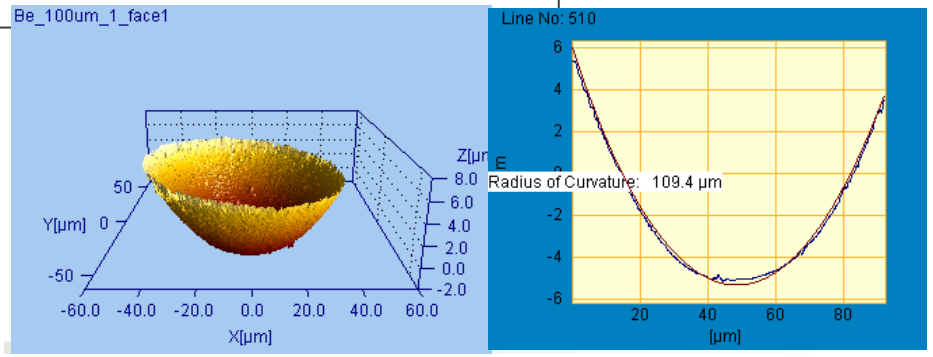

Be-CRL Focusing & Transparency Test at the APS

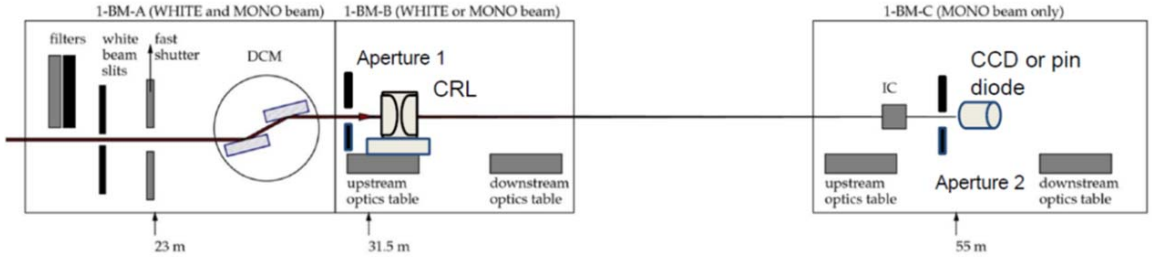

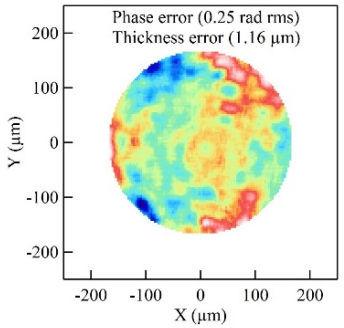

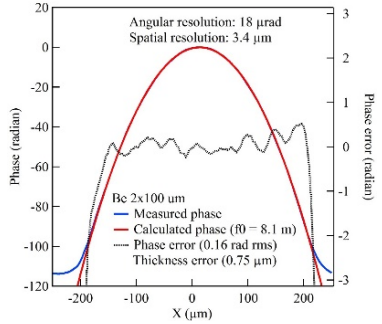

- Transmission of a Be-CRL of f=50 m (from Lengeler) was tested to be close to 99%
- Wavefront measurement data shows < 1 μm surface error
- **Be-CRL endurance under intense x-ray exposure was demonstrated as a by-product of the diamond endurance test (25 μ thick Be window exposed to 3 kW/mm^2 x-rays)!**

S. Stoupin, J. Kryziwinski, T. Kolodziej, D. Shu, X. Shi, Yu. Shvyd'ko, Kim K-J. (2016) t.b.p

Reflectivity of Si in Bragg Backscattering

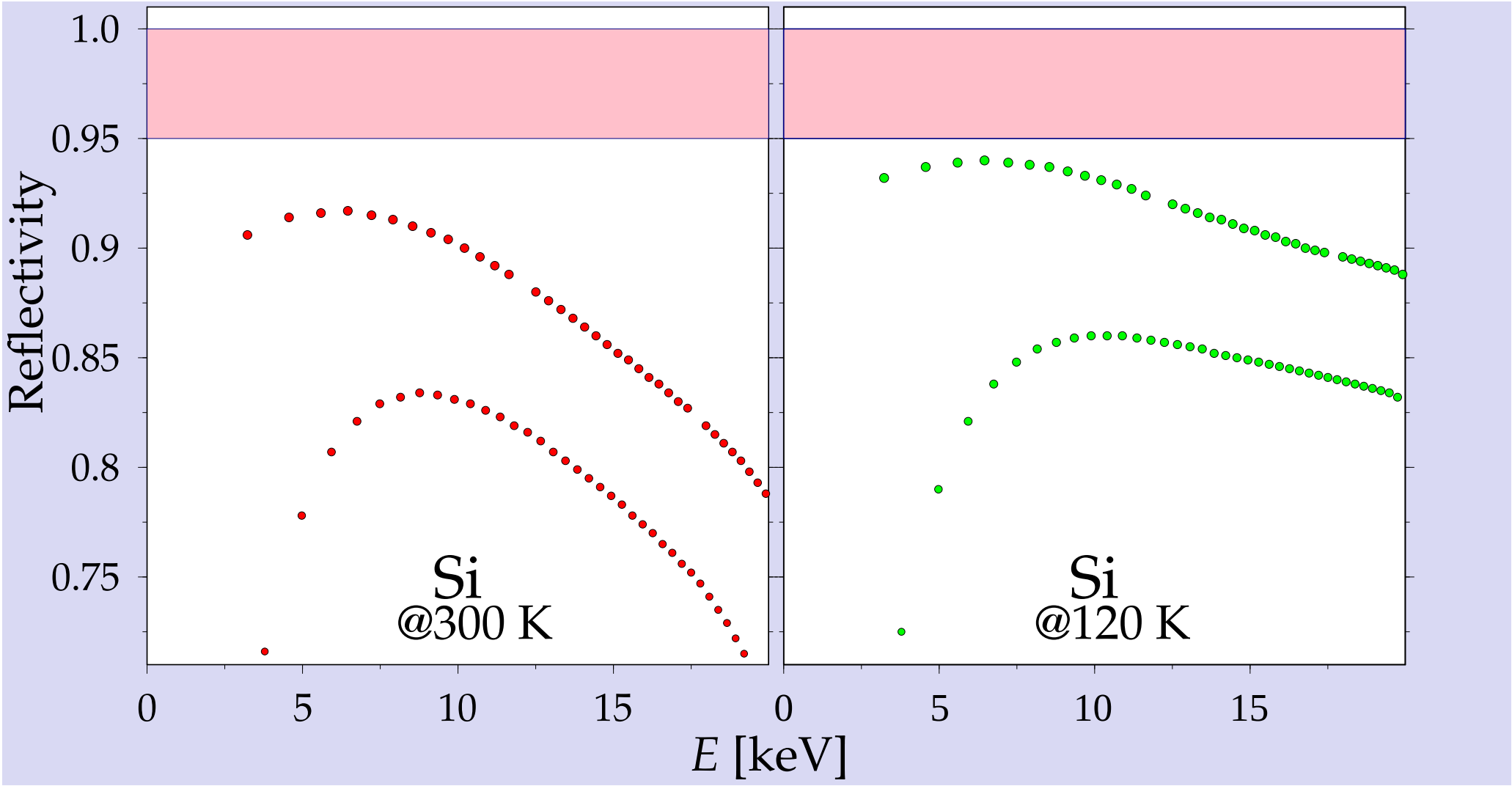

Theory: Highest Bragg Reflectivity from Diamond

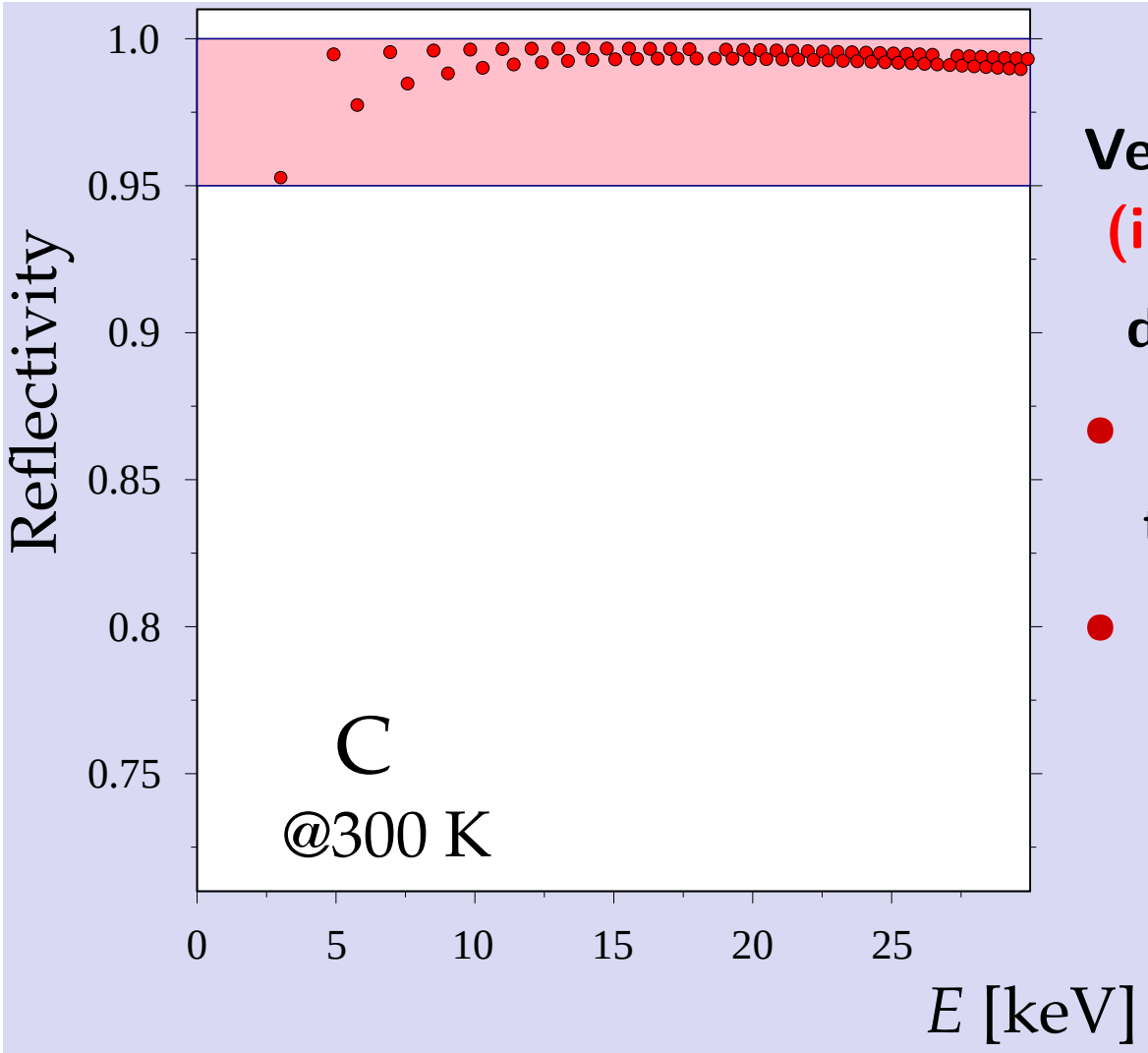

Very high reflectivity $\gtrsim 98 - 99\%$
(in theory)

due to:

- **High Debye Temperature, and thus high Debye-Waller factor**
- **Low Z, low photo absorption**

Diamond: superlative physical properties

Record high reflectivity

for hard x-rays

Theory: $> 99\%$

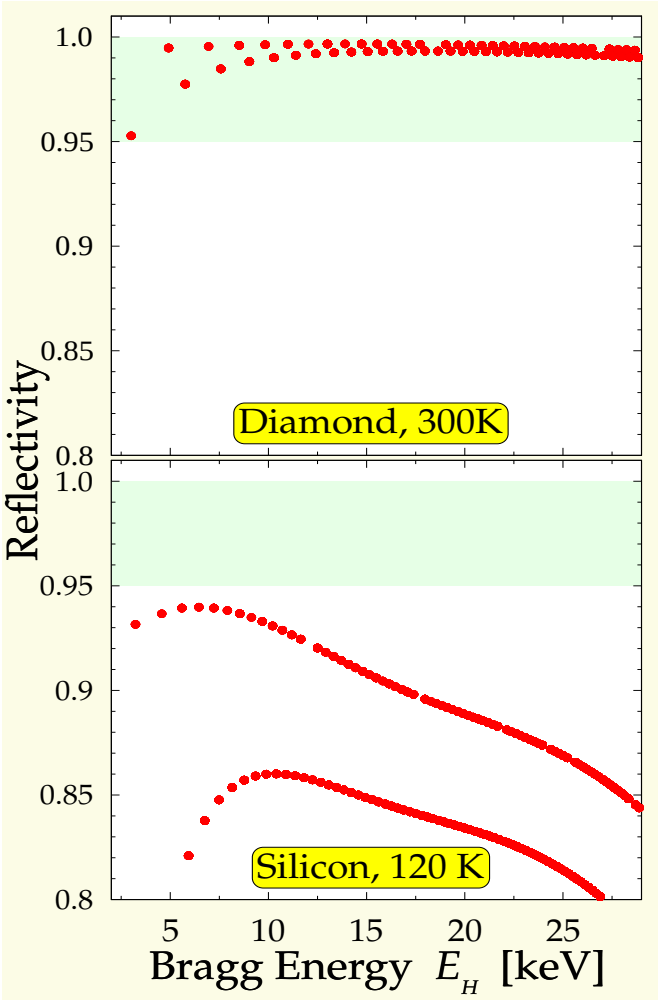

Yu. Shvyd'ko et al Nature Phys. (2010)

Diamond: superlative physical properties

Record high reflectivity for hard x-rays

Theory: $> 99\%$

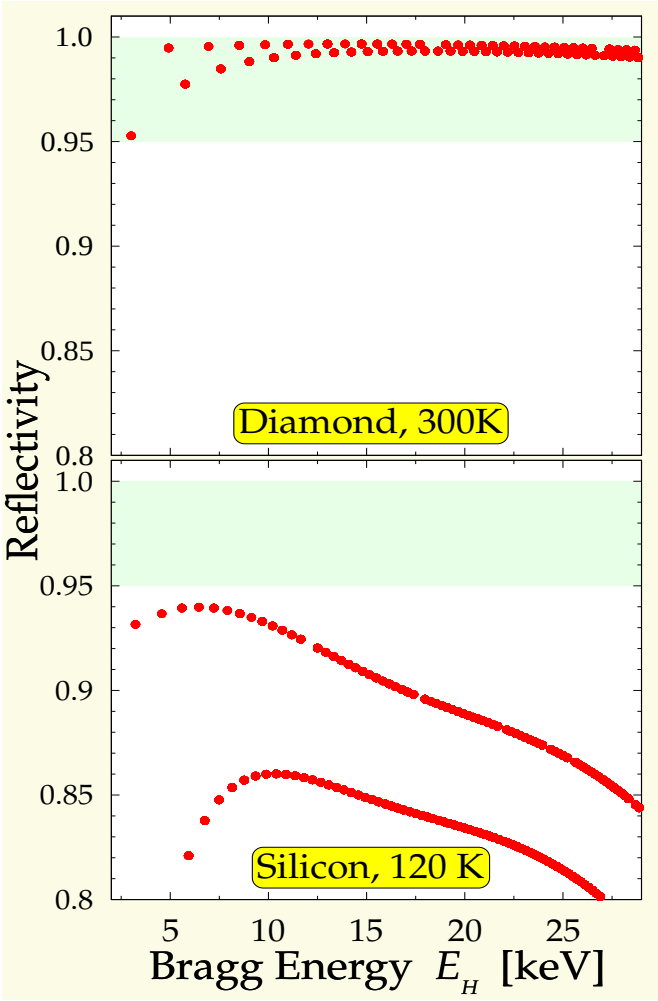

Yu. Shvyd'ko et al Nature Phys. (2010)

Ultra-high thermal diffusivity at low temperatures

$\simeq 10^5$ mm^{-2}s @ 100 K

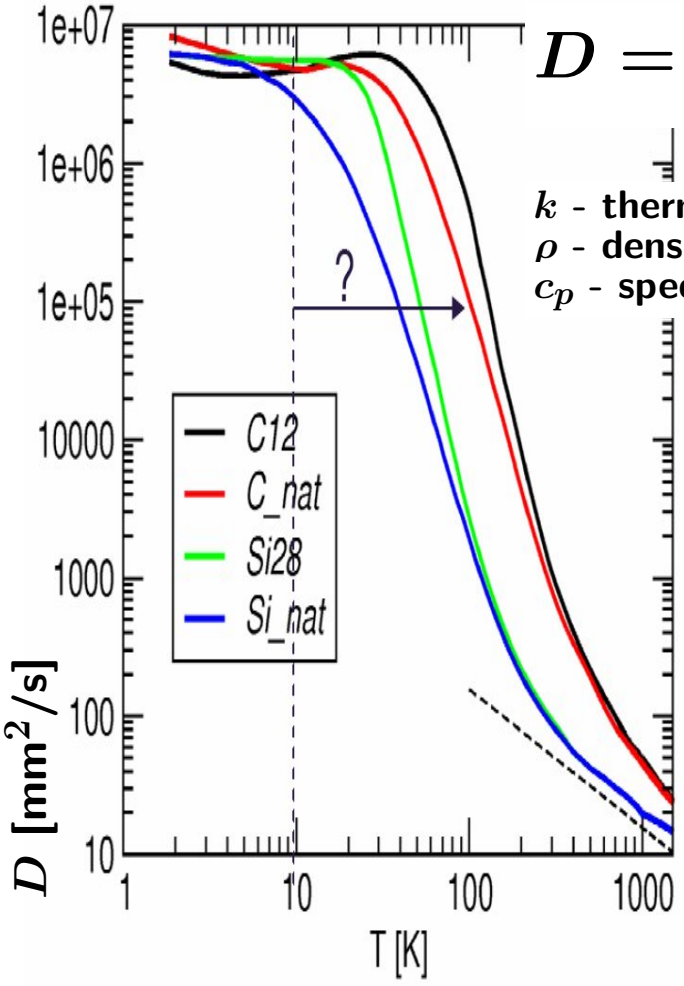

$$D = \frac{k}{\rho c_p}$$

k - thermal conductivity
ρ - density
c_p - specific heat capacity

Courtesy of H. Sinn

Diamond: superlative physical properties

Record high reflectivity for hard x-rays

Theory: $> 99\%$

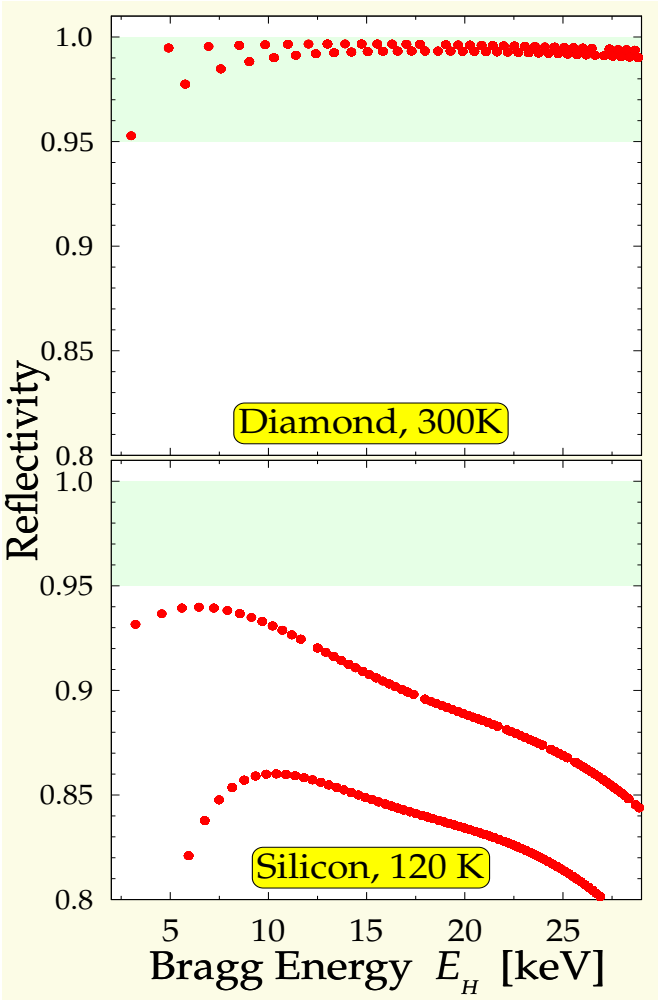

Yu. Shvyd'ko et al Nature Phys. (2010)

Ultra-high thermal diffusivity at low temperatures

$\simeq 10^5$ mm^{-2}s @ 100 K

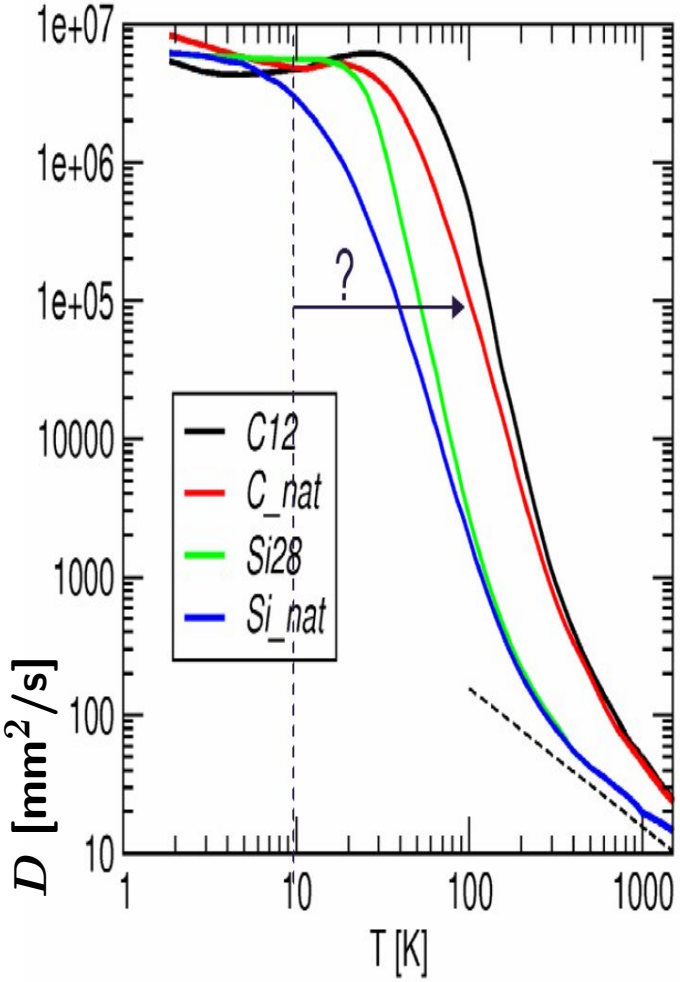

Courtesy of H. Sinn

Ultra-low thermal expansion at low temperatures

$\simeq 10^{-8}$ K^{-1} @ 100 K

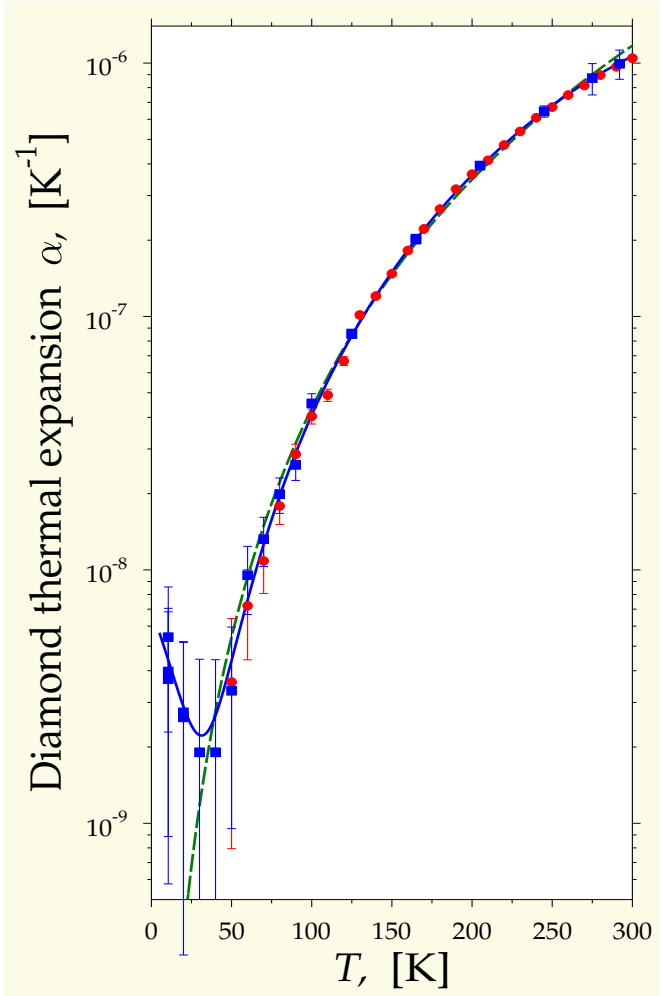

S. Stoupin, Yu. Shvyd'ko PRL (2010)

Quality and Reflectivity of Diamond Crystals

20 Years Ago ...

IIa, HTHP, from GE

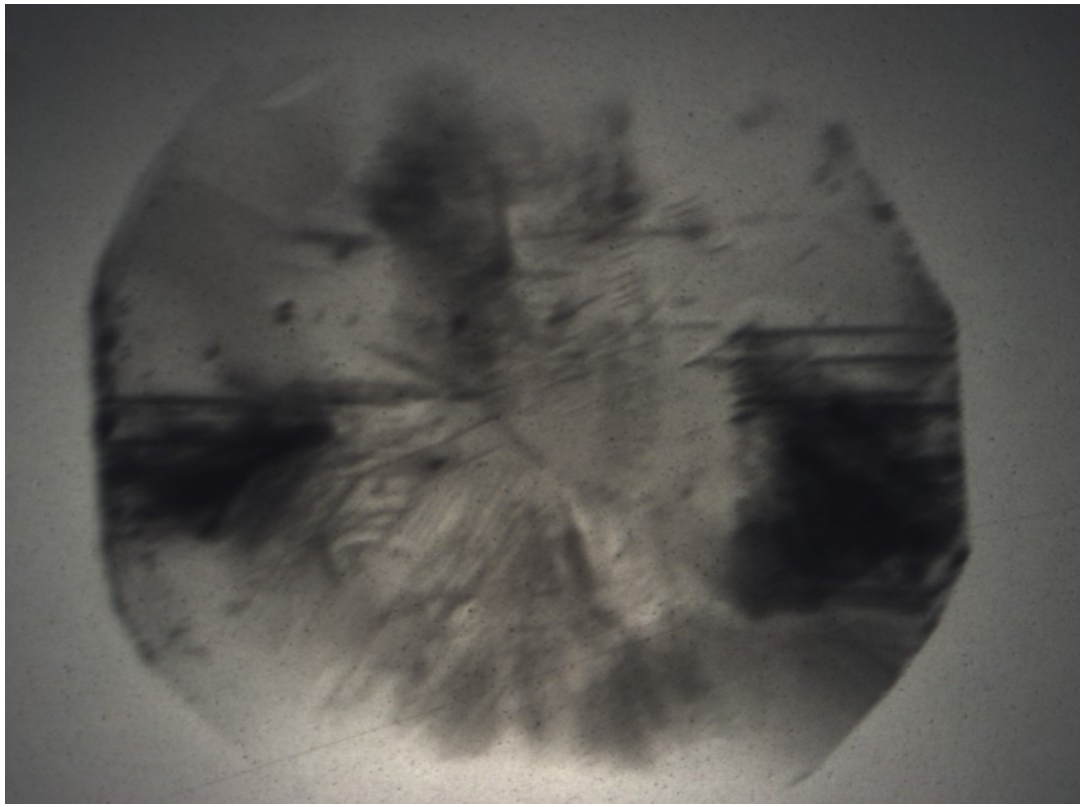

(f) $\bar{3}\bar{1}1$

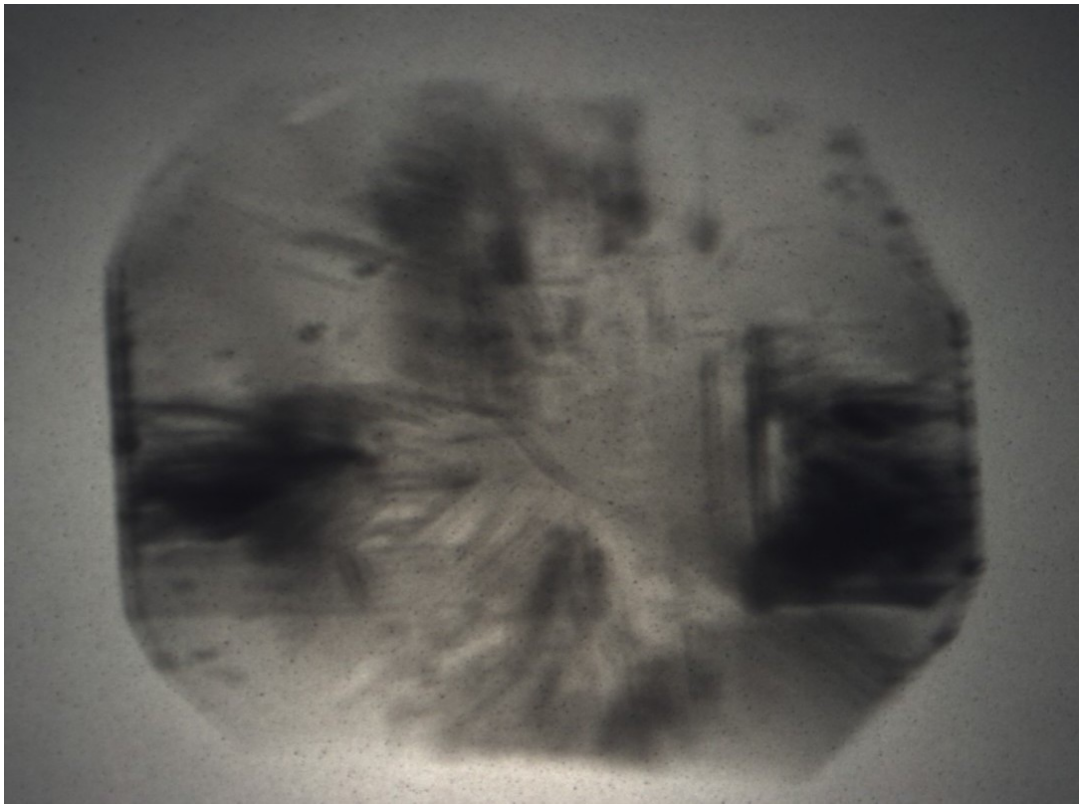

(g) $\bar{3}11$

x-ray white beam topography: Stoupin, 2011 (APS)

Diamond Crystal Quality. State of the Art

Progress in fabrication, characterization, and X-ray optics applications of synthetic high-quality HTHP diamond of type-IIa was substantial in the last two decades:
Pal'yanov et al. (1990), Berman et al. (1993), Freund (1995), Sumiya and Satoh (1996), Fernandez et al. (1997), Sellschop et al. (2000), Sumiya et al. (2000), Zhong et al. (2007), Yabashi et al. (2007), Burns et al. (2009), Polyakov et al. (2011).

Crystals with $> 4 \times 4$ mm^2 defect-free areas Burns et al. (2009), Polyakov et al. (2011) is the state of the art.

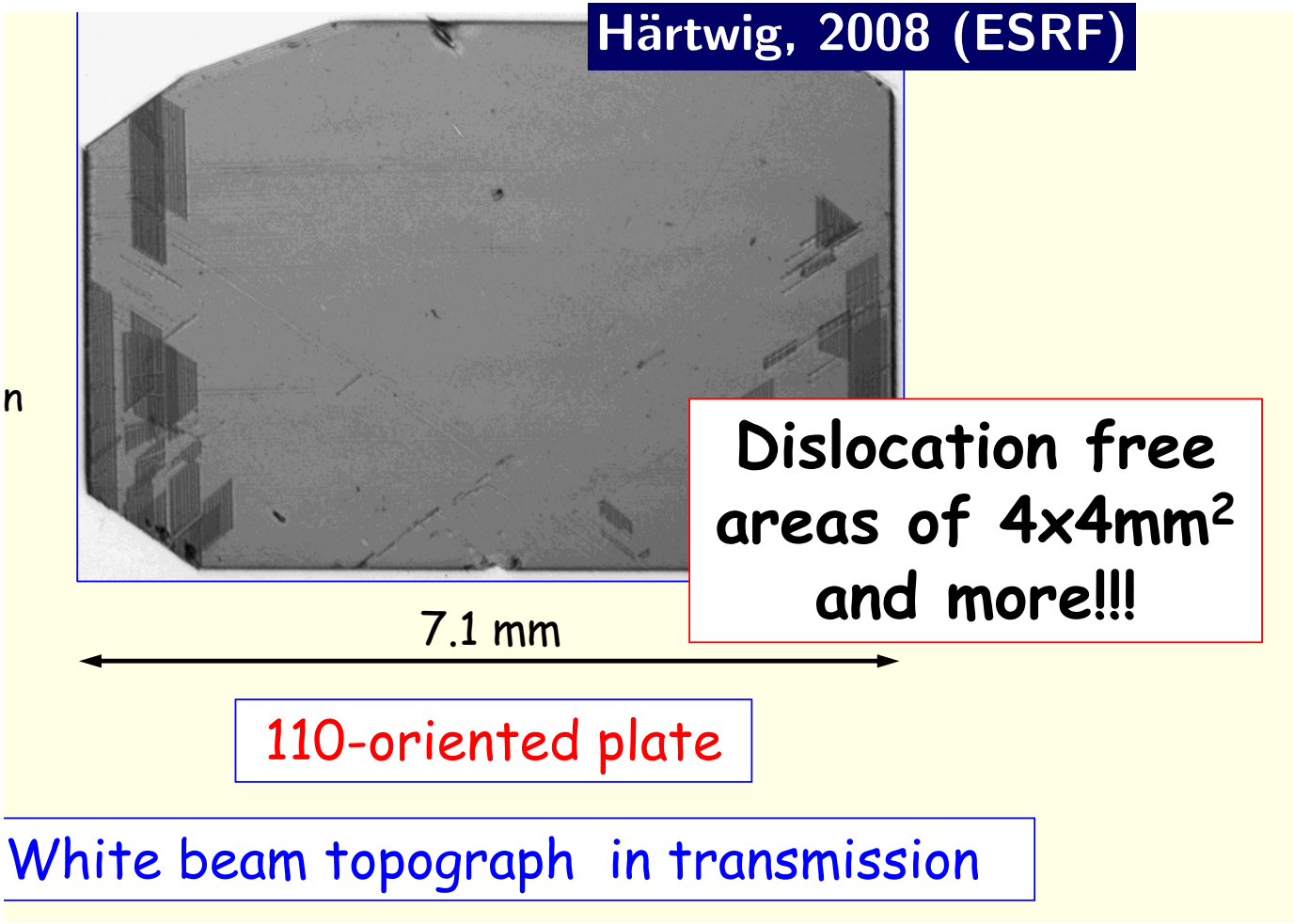

High Quality Diamonds from Sumitomo

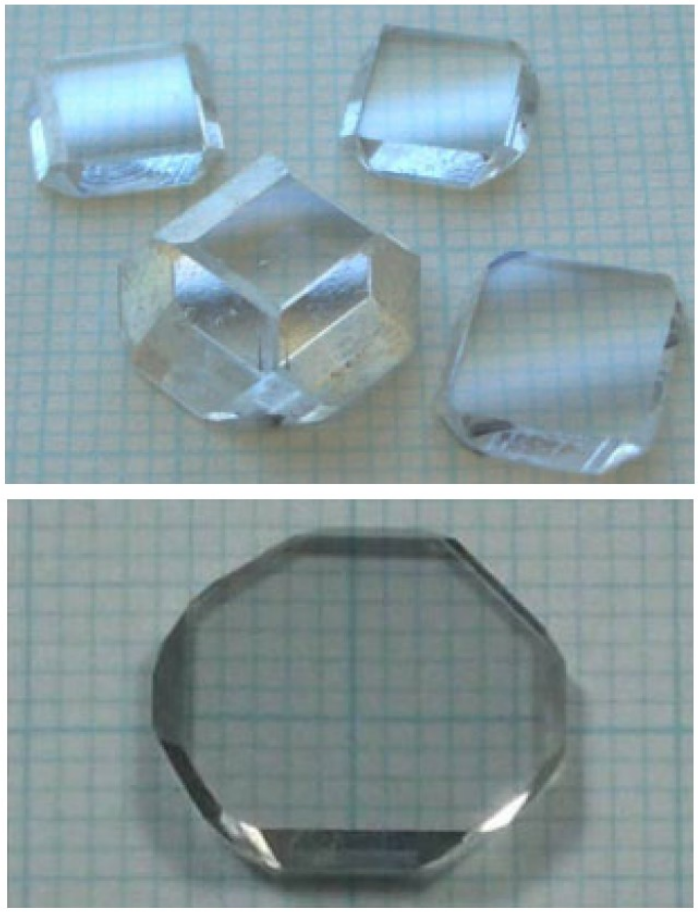

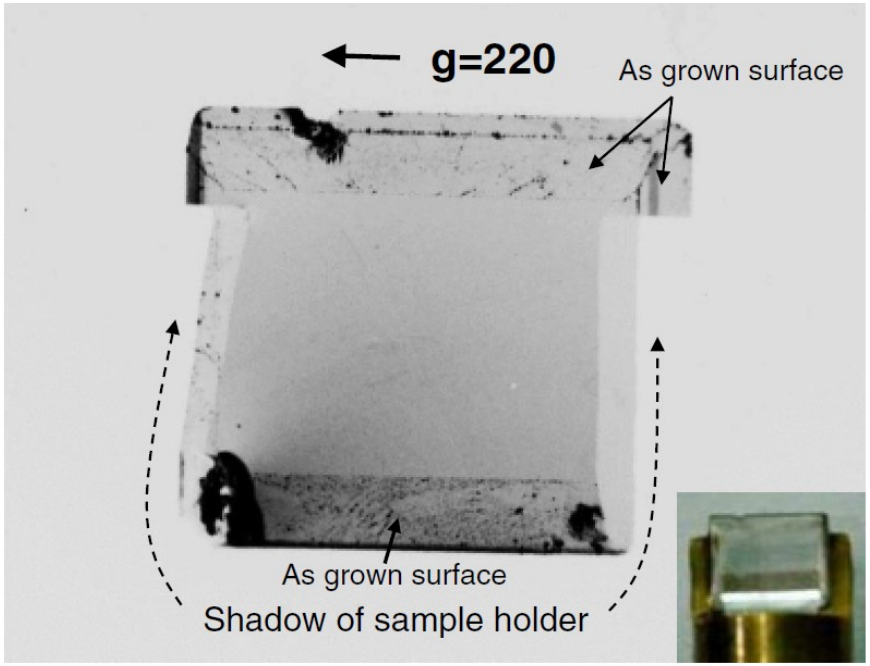

Fig. 5. (Color online) Transmission X-ray topograph of (001) diamond plate shown in Fig. 4(a) ($7.5 \times 6 \times 0.7\,\mathrm{mm}^3$) cut from the upper region of a large synthetic type IIa diamond crystal. Bottom right shows the diamond plate attached to the sample holder for topography measurement.

Fig. 3. (Color online) Large synthetic type IIa diamond crystals. Bottom: the largest diamond plate prepared from a large crystal of 12 mm diameter.

Sumiya & Tamasaku JJAP 51 (2012) 090102

Courtesy of Kenji Tamasaku

Isotope-Pure Diamonds

^{12}C 99.999% ⟷ ^{12}C: 98.9%
^{13}C: 1.1%

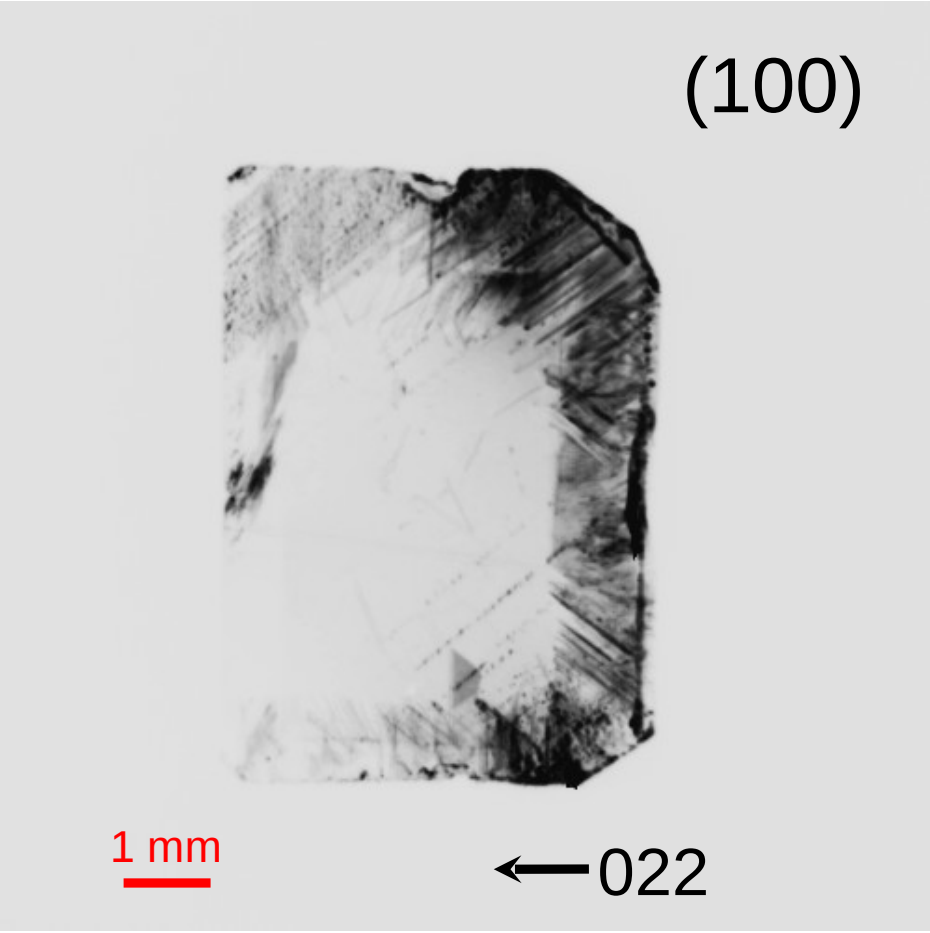

Transmission topograph
Si331(b=20.9) - C220 @14.55 keV

Thermal conductivity x3(?) of ^{Nat}C

For ultra-high heat-load optics

H. Sumiya, K. Harano, K. Tamasaku, unpublished

Courtesy of Kenji Tamasaku

Type-IIa, HTHP Diamond from TISNCM (I)

Visible light image

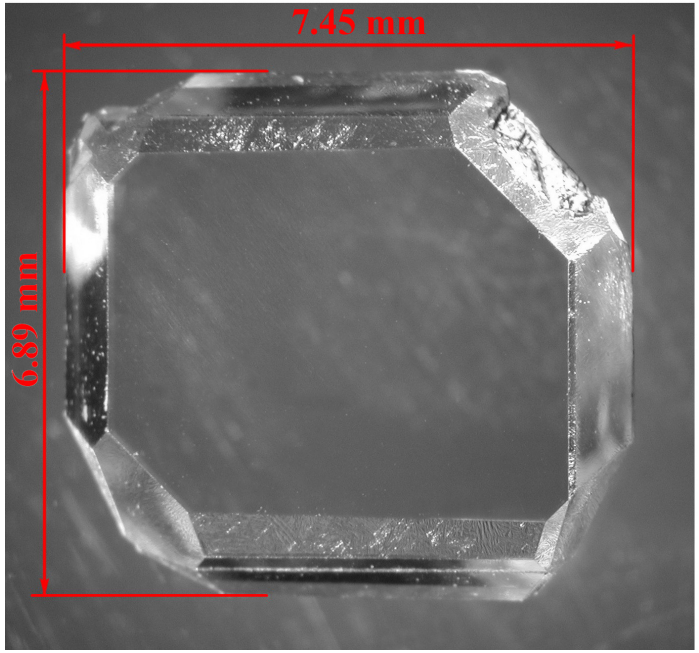

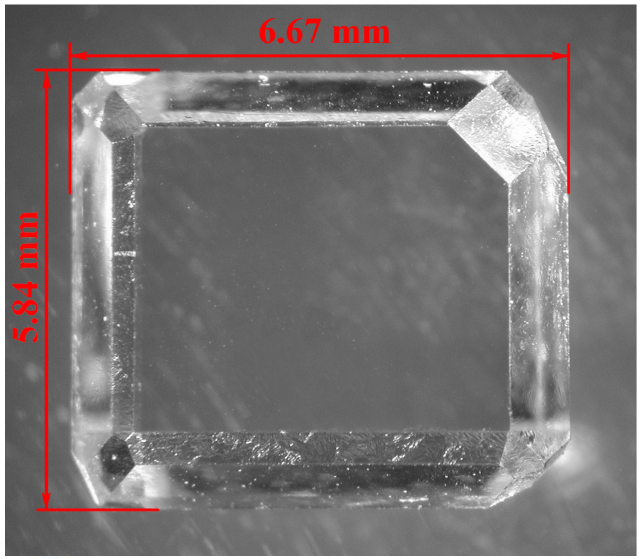

X-ray Lang topography in transmission

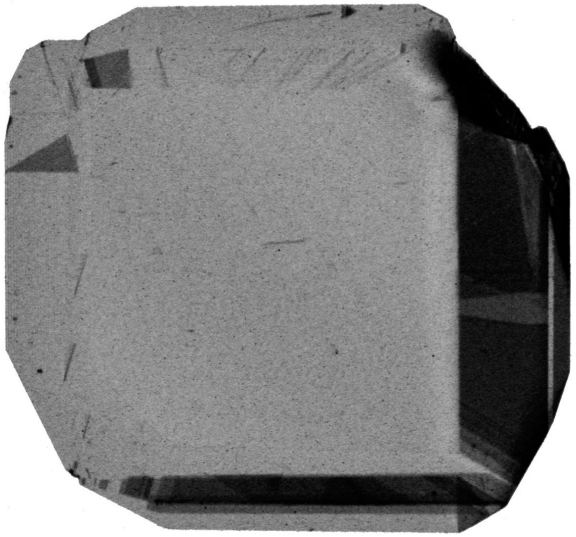

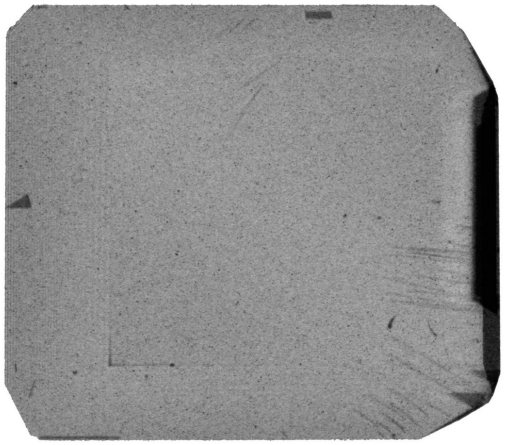

Blank, Terentyev, et al.

Technological Institute for Superhard and New Carbon Materials (TISNCM)
Troitsk, Russia

Preselected diamond plates:

(001) orientation, 1mm thick

dislocation & stacking fault free areas $> 4 \times 4$ mm^2 and more

Diamond Reflectivity Studies: C(008) @ 14.3 keV

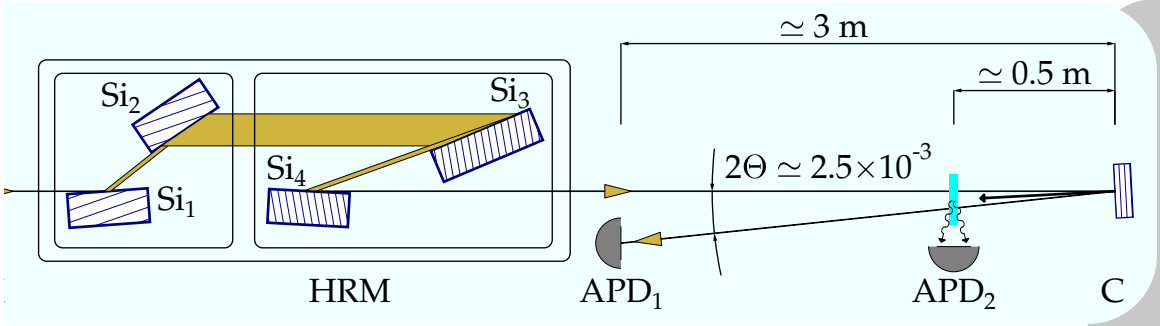

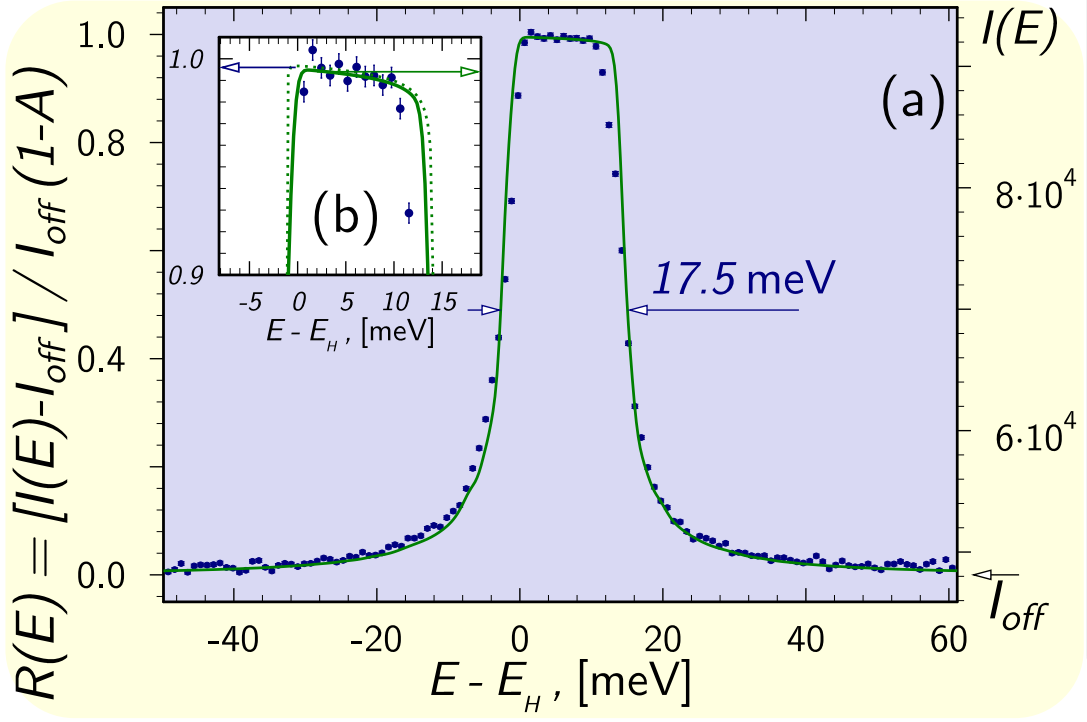

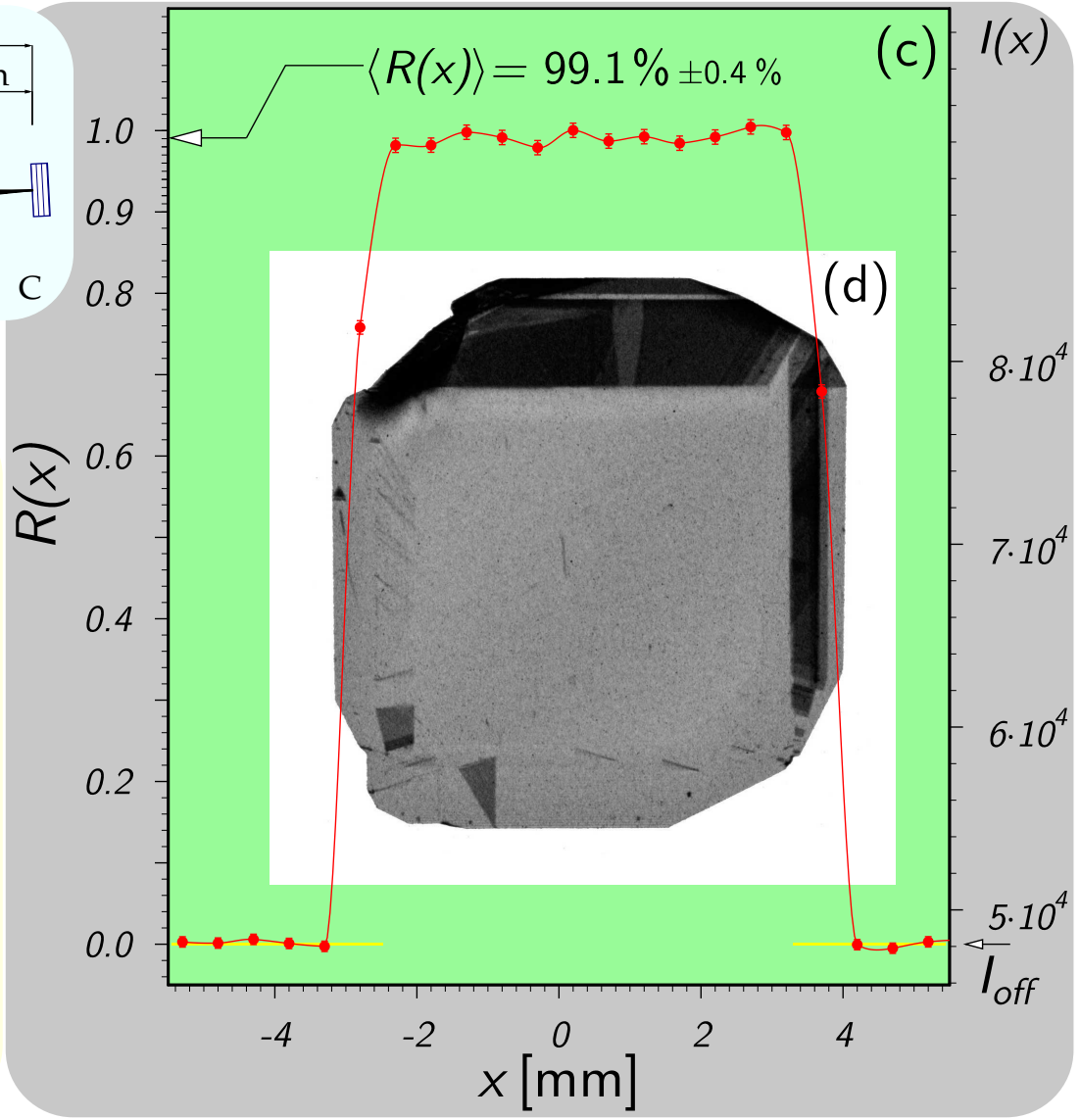

Shvyd'ko, Stoupin, Blank, Terentyev, Nature Photonics 5 (2011) 539

Diamond Reflectivity Studies: C(008) @ 14.3 keV

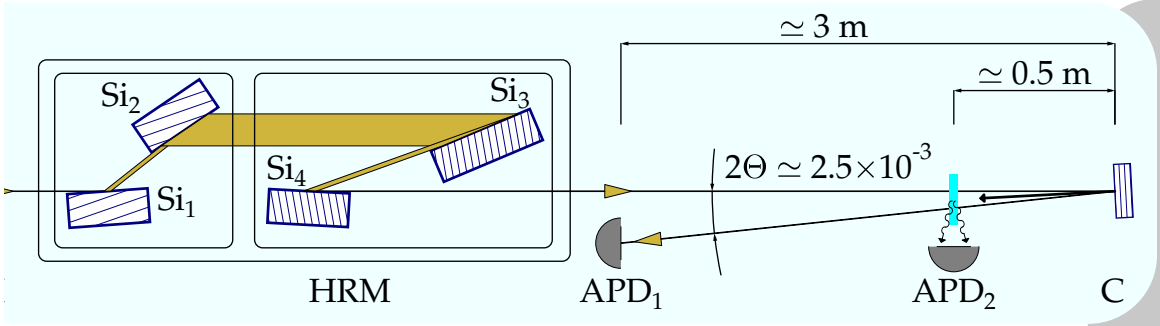

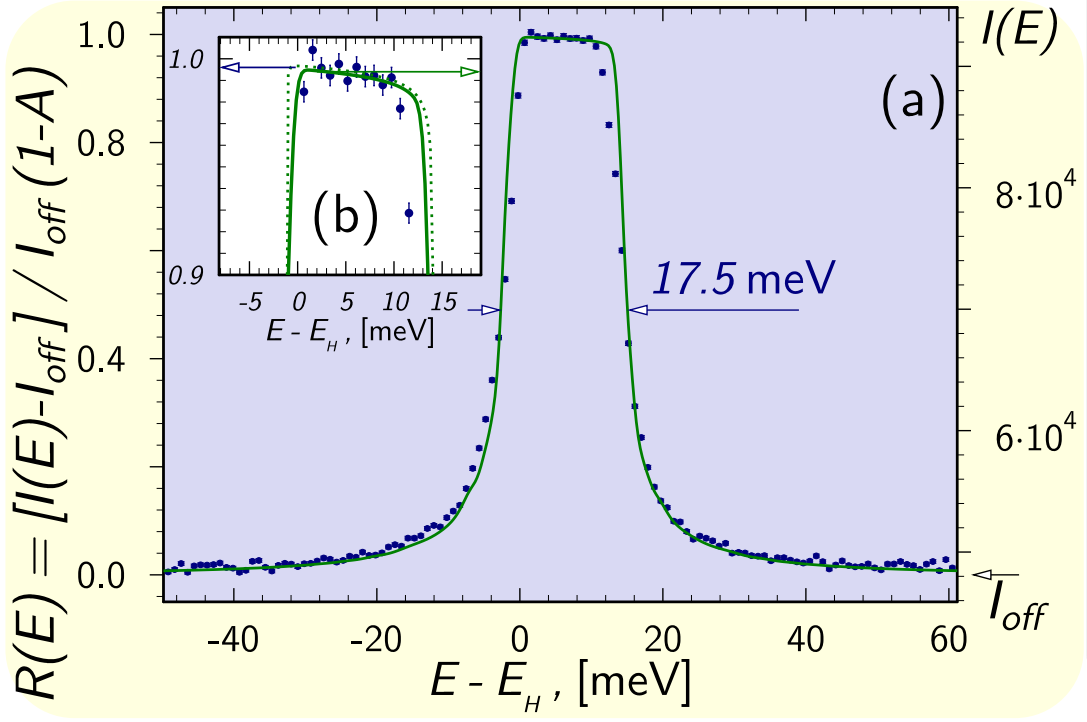

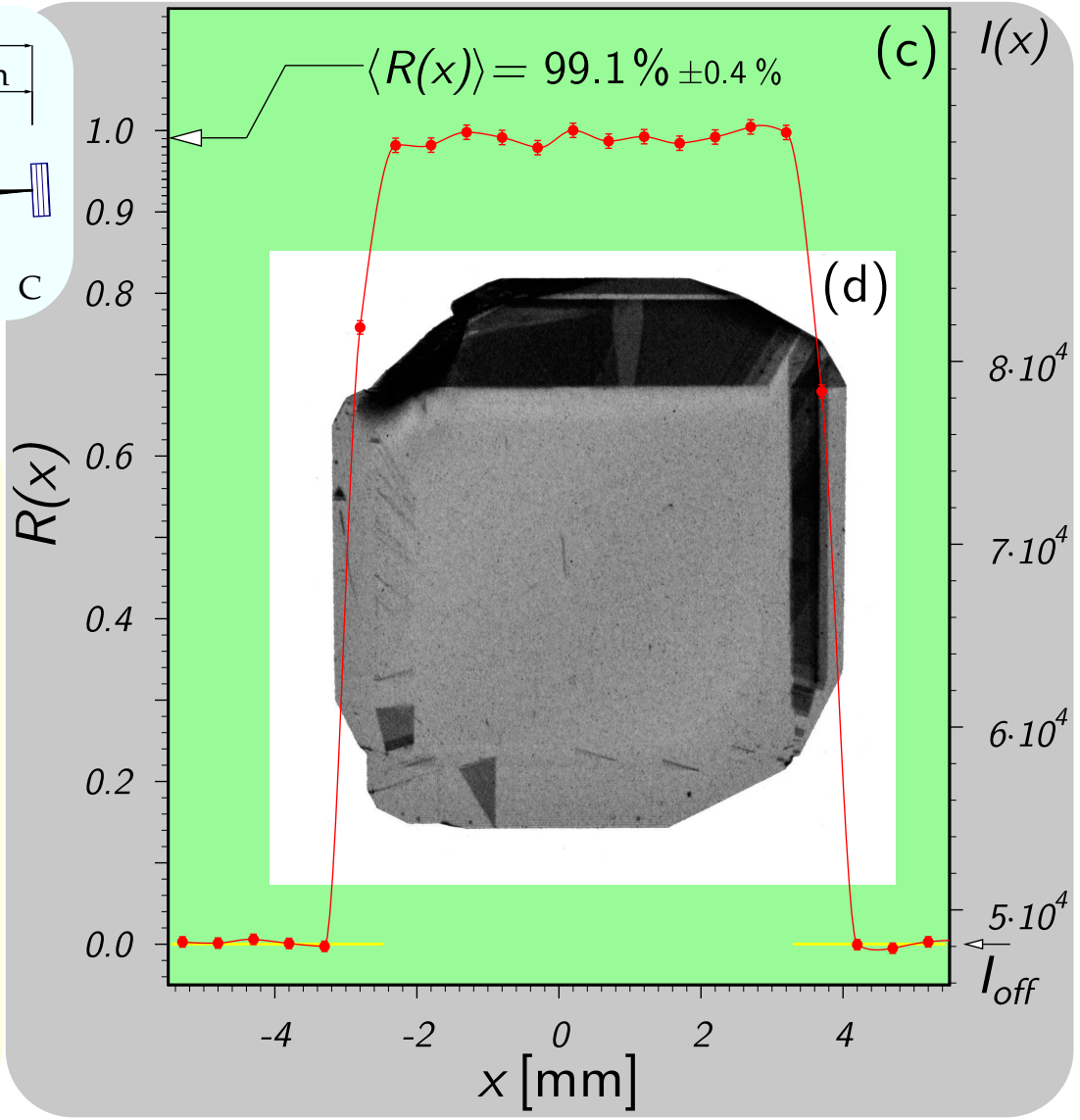

Shvyd'ko, Stoupin, Blank, Terentyev, Nature Photonics 5 (2011) 539

$\simeq 99\%$ reflectivity and close to theoretical performance.

meV-Bandwidth: C(13 3 3) @ E=23.7 keV

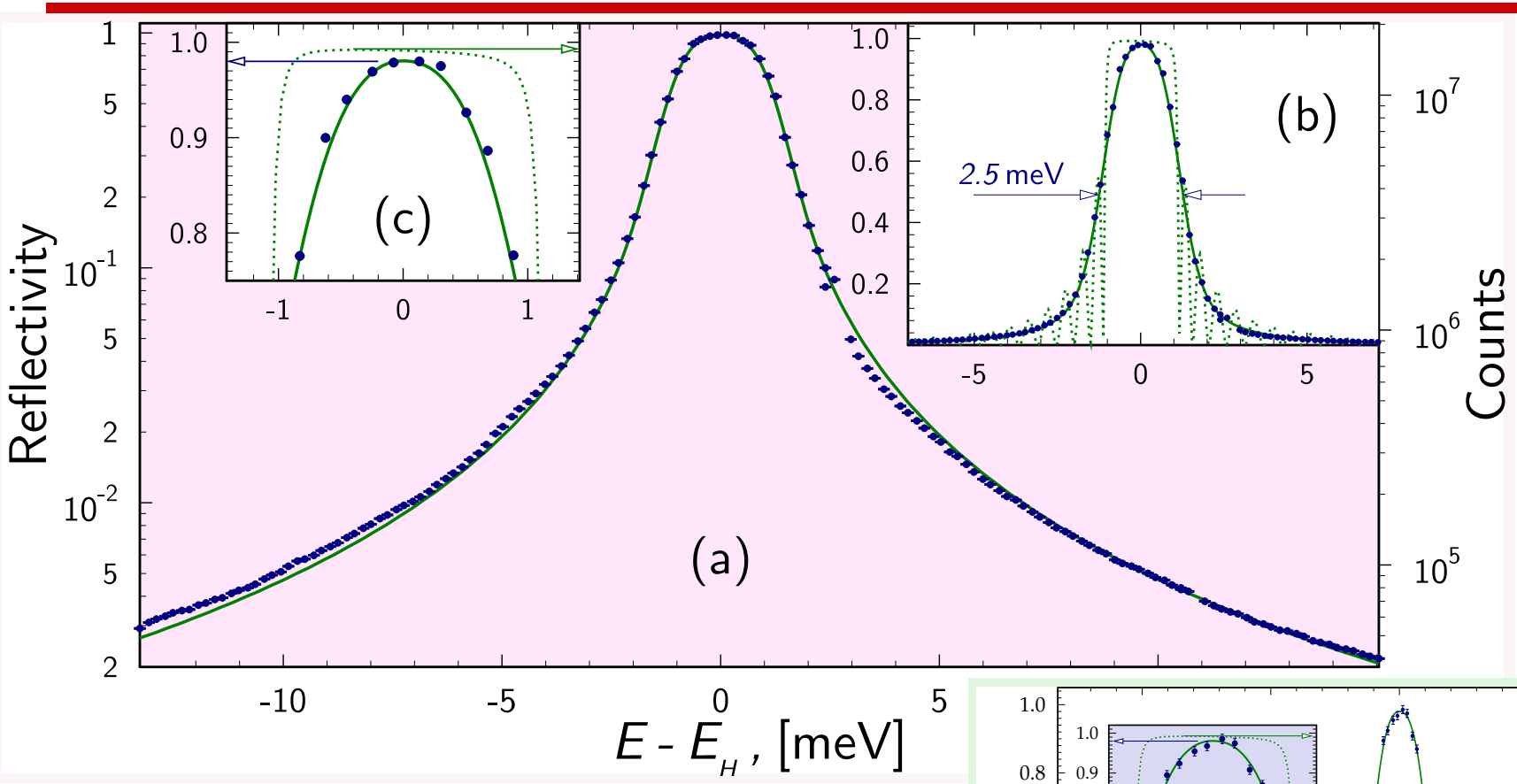

Measured 98% $\Longrightarrow$ 99%

with instrumental function taken into account

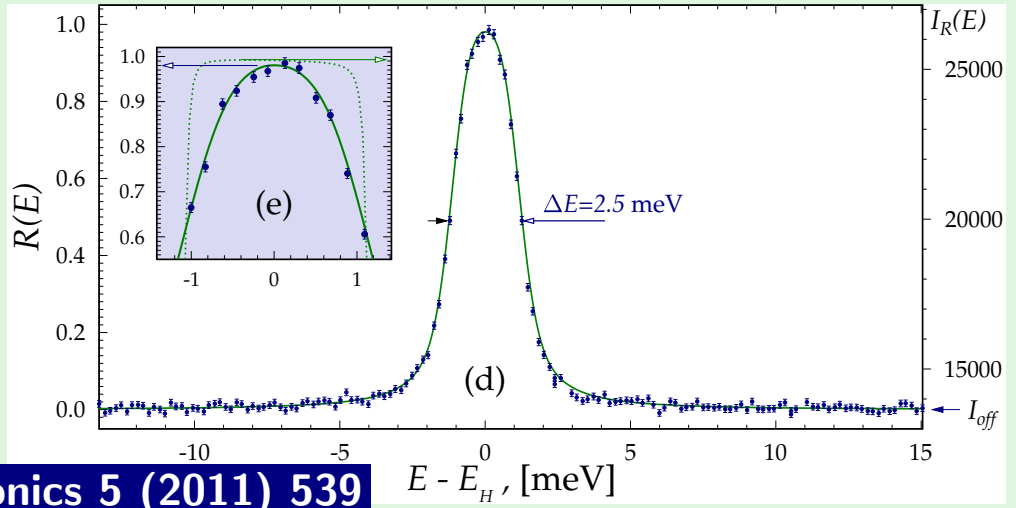

Shvyd'ko, Stoupin, Blank, Terentyev, Nature Photonics 5 (2011) 539

meV-Bandwidth: C(13 3 3) @ E=23.7 keV

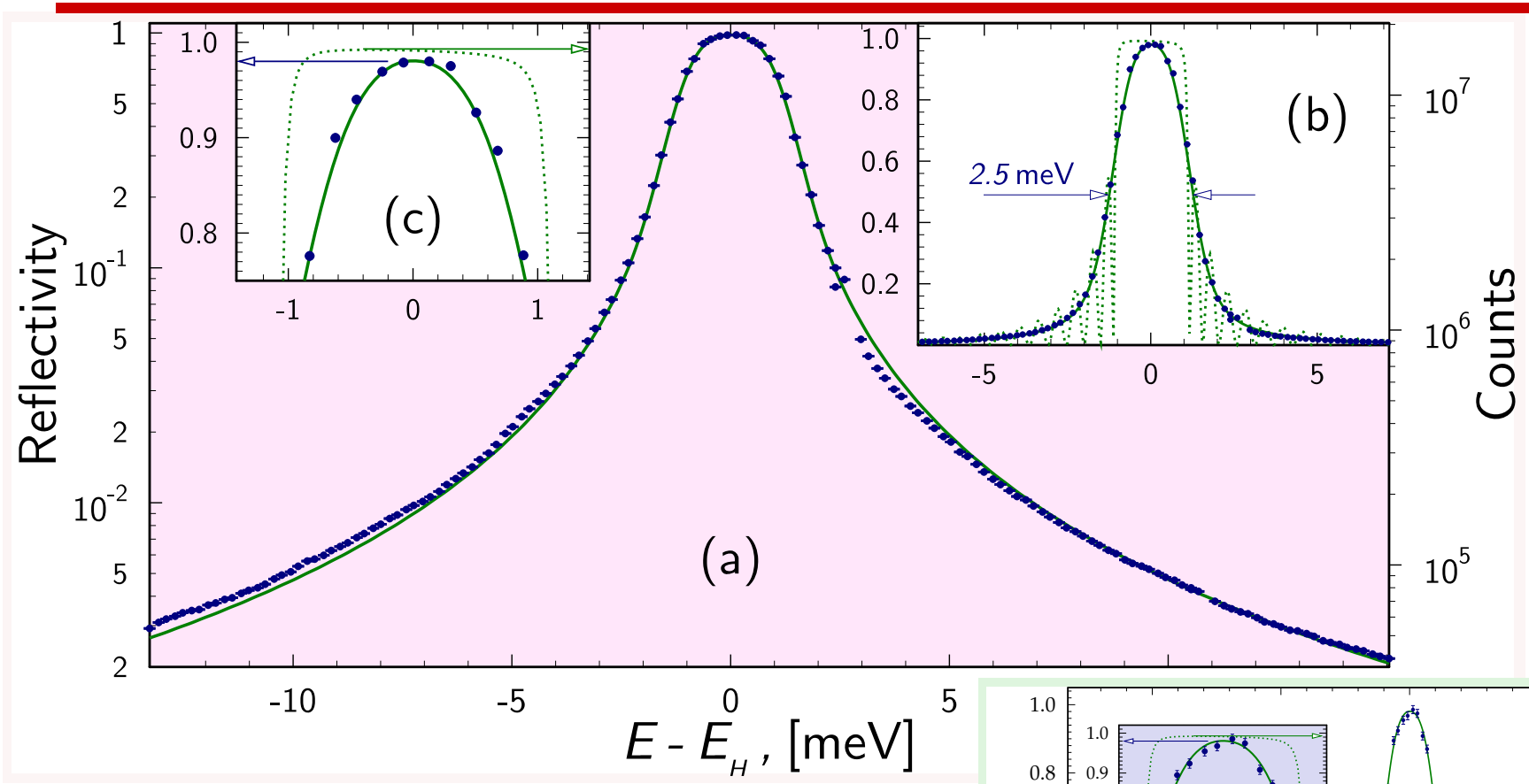

Measured $98\% \implies 99\%$

with instrumental function taken into account

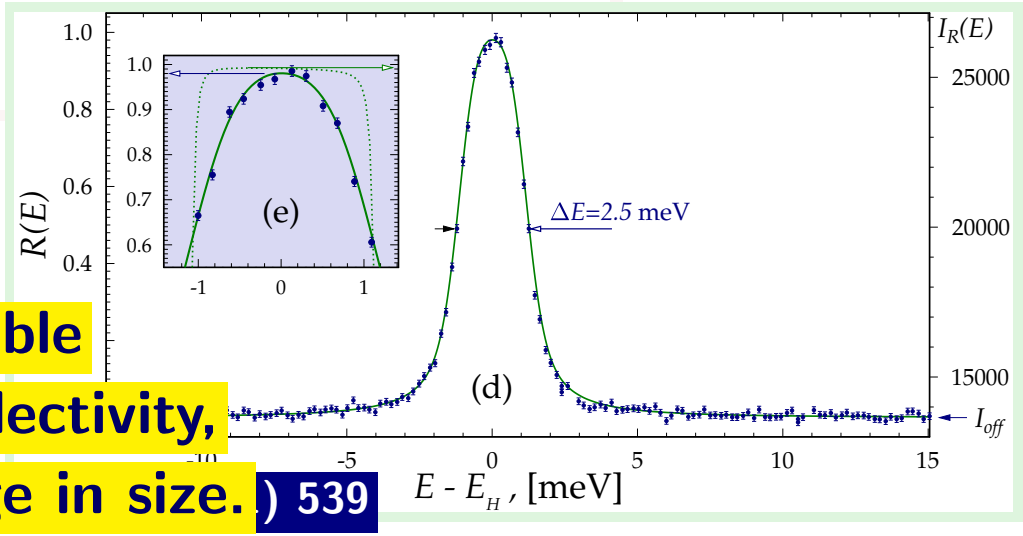

Synthetic diamond crystals are available showing almost theoretically high reflectivity, small bandwidth, and sufficiently large in size.) 539

meV-Bandwidth: C(13 3 3) @ E=23.7 keV

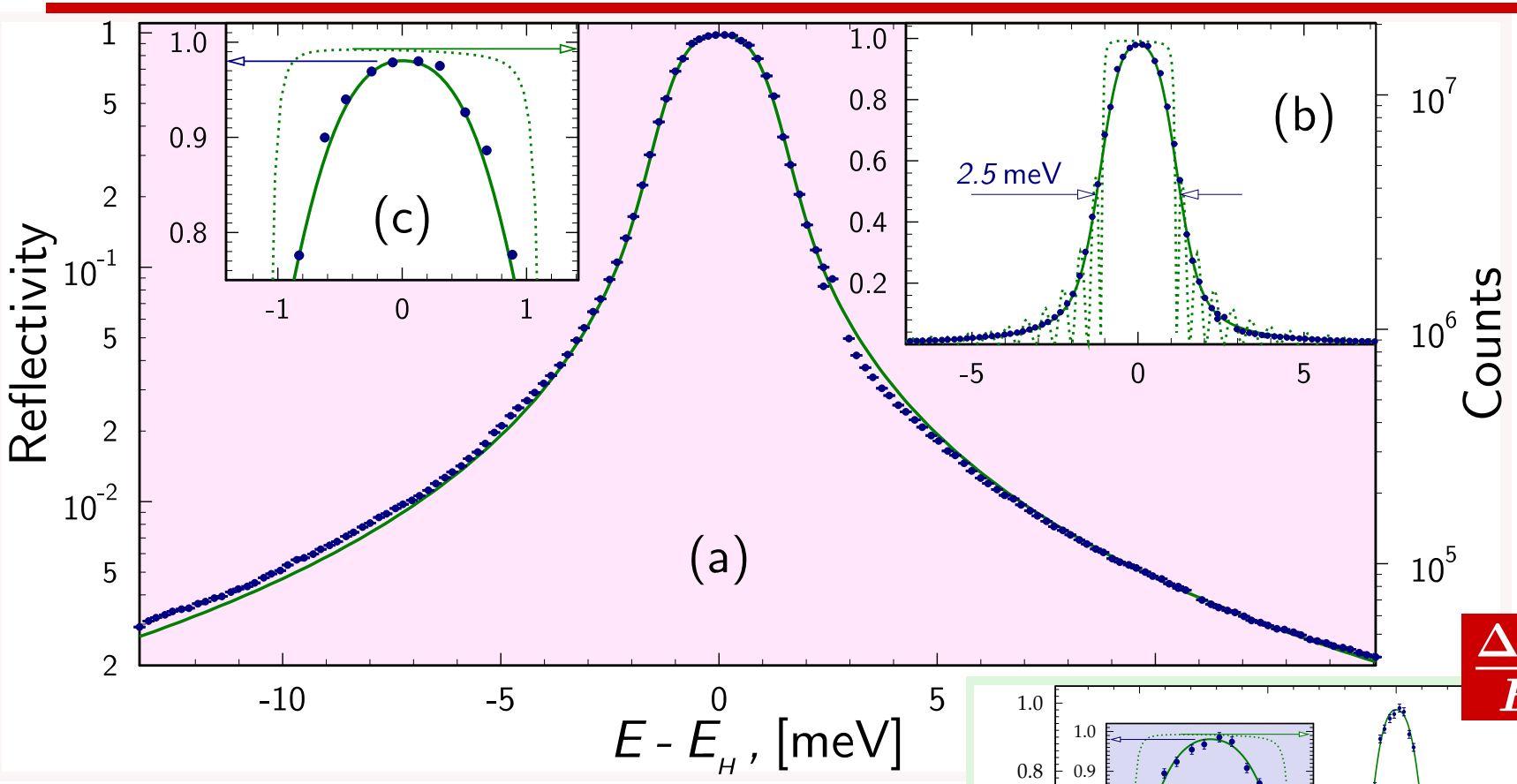

$$\frac{\Delta E}{E} \simeq 10^{-7}$$

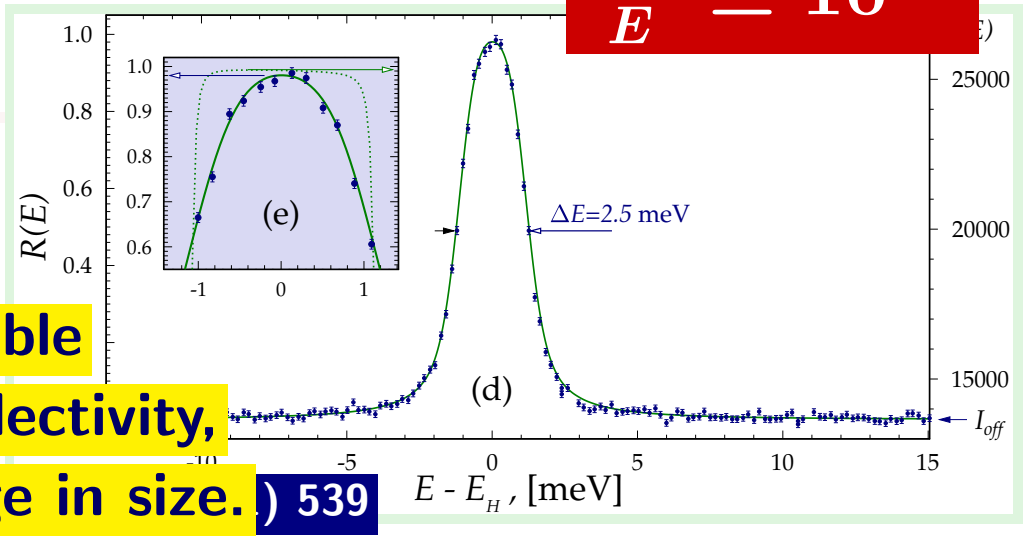

Measured $98\% \implies 99\%$

with instrumental function taken into account

Synthetic diamond crystals are available showing almost theoretically high reflectivity, small bandwidth, and sufficiently large in size.) 539

Outcoupling through Thin Diamond Crystals

A few tens of microns thick perfect diamond single crystals, properly functioning under Bragg diffraction conditions are required for outcoupling of x-rays.

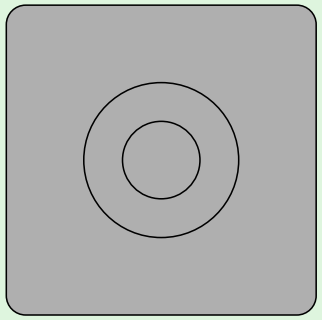

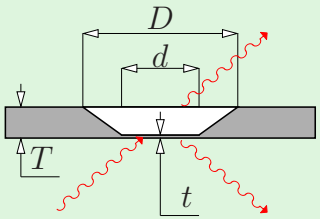

Drumhead crystals, monolithic crystal structures comprised of a thin membrane furnished with a surrounding solid collar, are a solution ensuring mechanically stable strain-free mounting of the membranes with efficient thermal transport.

Almost flawless diamond drum-head crystal with a 25 μm thin membrane in the (100) orientation manufactured by picosecond laser milling.

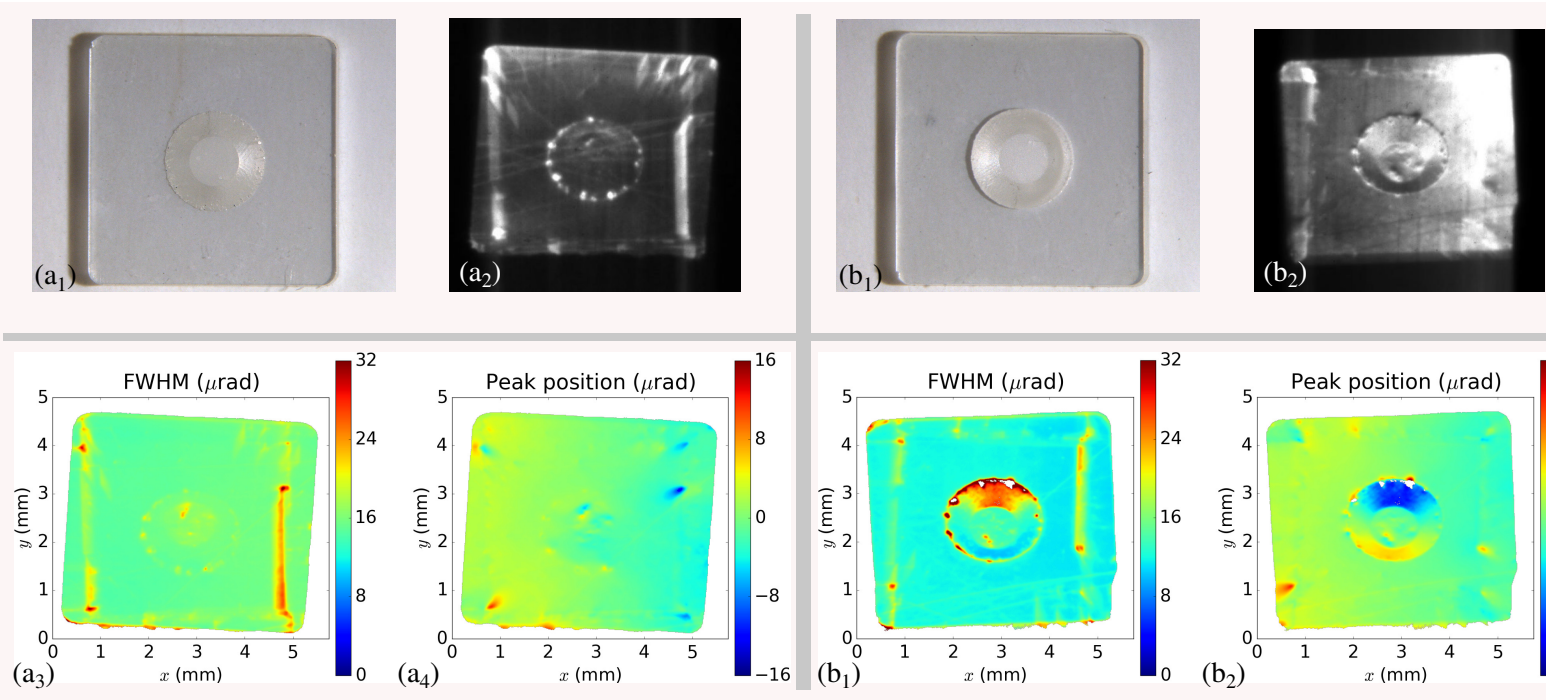

Kolodziej, Vodnala, Terentyaev, Blank & Shvyd'ko (2016) J. Appl. Cryst. 49

Heat Load Problem

Heat Load Problem

Temperature gradient $\delta T \Rightarrow$ r.c. energy spread $\delta E/E = \beta \delta T$.
Requirement: $\delta E \lesssim 1$ meV, when the next pulse arrives.

Incident power $\simeq 50$ μJ/pulse.

Absorbed power: $\simeq 1$ μJ/pulse (2%).

Footprint: $\simeq 100 \times 100$ μm^2

Is it a problem?

Heat Load Problem

Temperature gradient $\delta T \Rightarrow$ r.c. energy spread $\delta E/E = \beta \delta T$.

Requirement: $\delta E \lesssim 1$ meV, when the next pulse arrives.

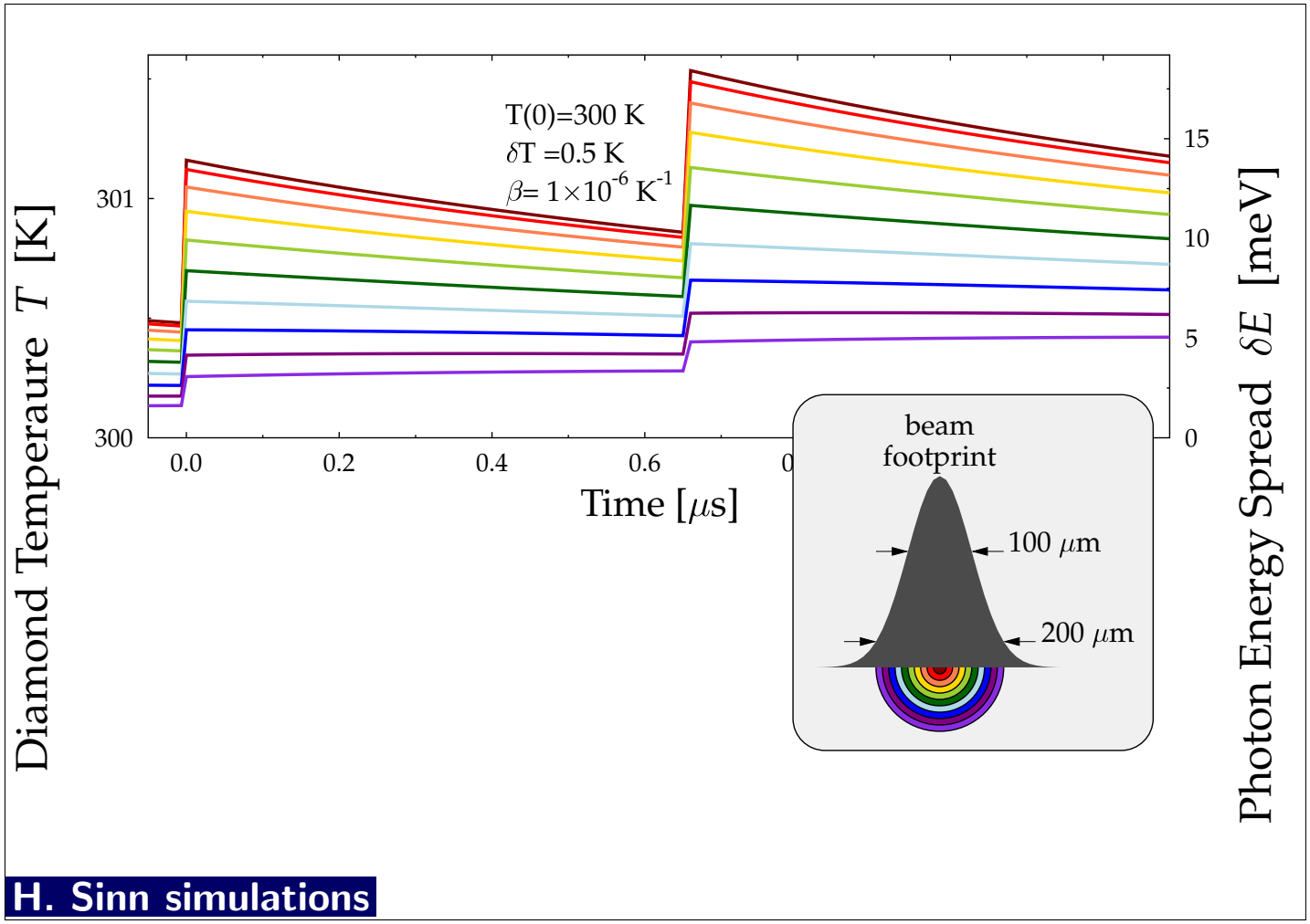

H. Sinn simulations

- **Big temperature jump δT after the x-ray pulse arrival.**
- **T=300K: Big temperature spread by the arrival of**

Heat Load Problem

Temperature gradient $\delta T \Rightarrow$ r.c. energy spread $\delta E/E = \beta \delta T$.

Requirement: $\delta E \lesssim 1$ meV, when the next pulse arrives.

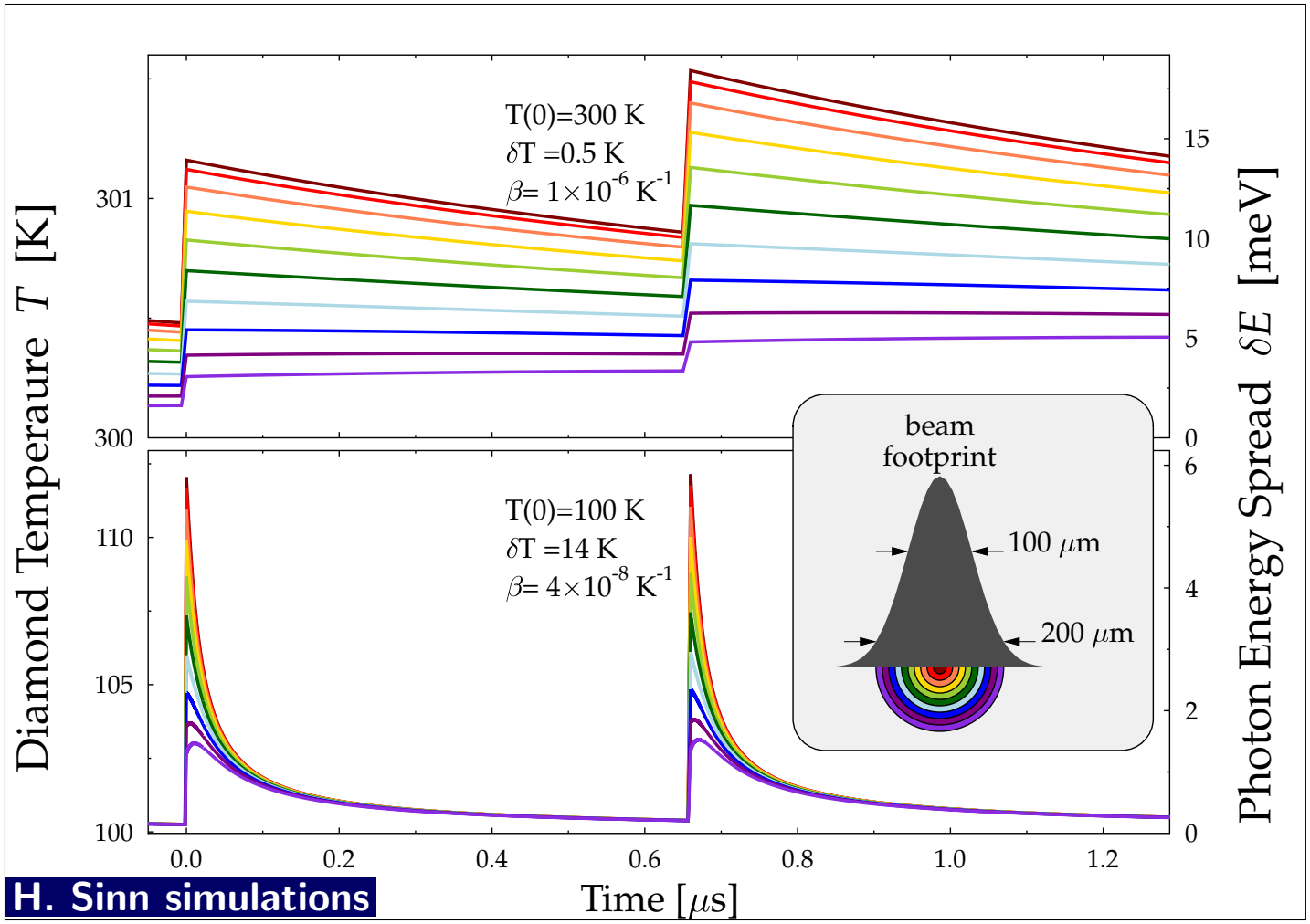

H. Sinn simulations

- **Big temperature jump δT after the x-ray pulse arrival.**
- **T=300K: Big temperature spread by the arrival of the next x-ray pulse.**
- **T=100K: Negligible temperature spread by the arrival of the next x-ray pulse.**

Heat Load Problem

Temperature gradient $\delta T \Rightarrow$ r.c. energy spread $\delta E/E = \beta \delta T$.

Requirement: $\delta E \lesssim 1$ meV, when the next pulse arrives.

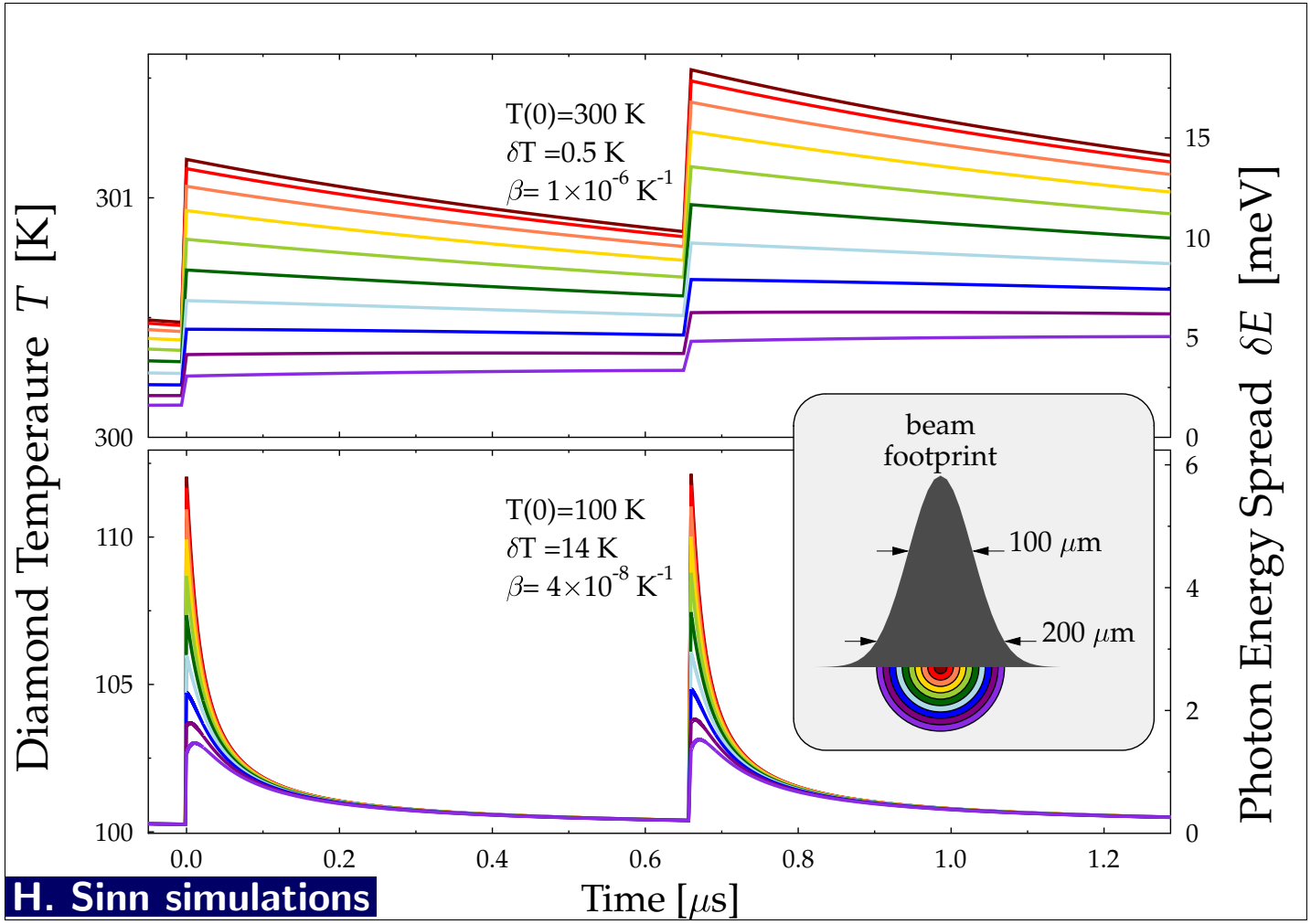

H. Sinn simulations

- Big temperature jump δT after the x-ray pulse arrival.
- T=300K: Big temperature spread by the arrival of the next x-ray pulse.
- T=100K: Negligible temperature spread by the arrival of the next x-ray pulse.
- Reasons:
  1. High temperature diffusivity $\mathcal{D}$
  2. Low temperature expansion β

Solution: **Maintain diamond at $T < 100$ K!**

Superb thermo-mechanical properties of diamond

Ultra-high thermal diffusivity at low temperatures

$$D = \frac{k}{\rho c_p}$$

k - thermal conductivity
ρ - density
c_p - specific heat capacity

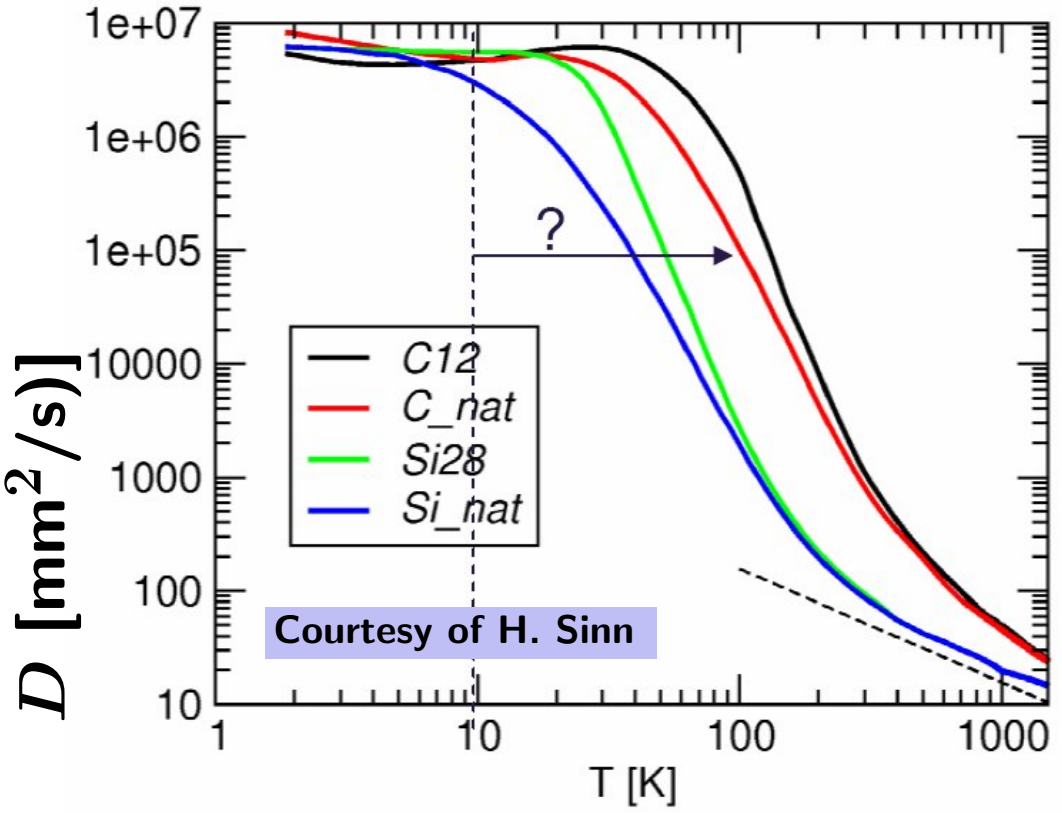

Ultra-low thermal expansion at low temperatures

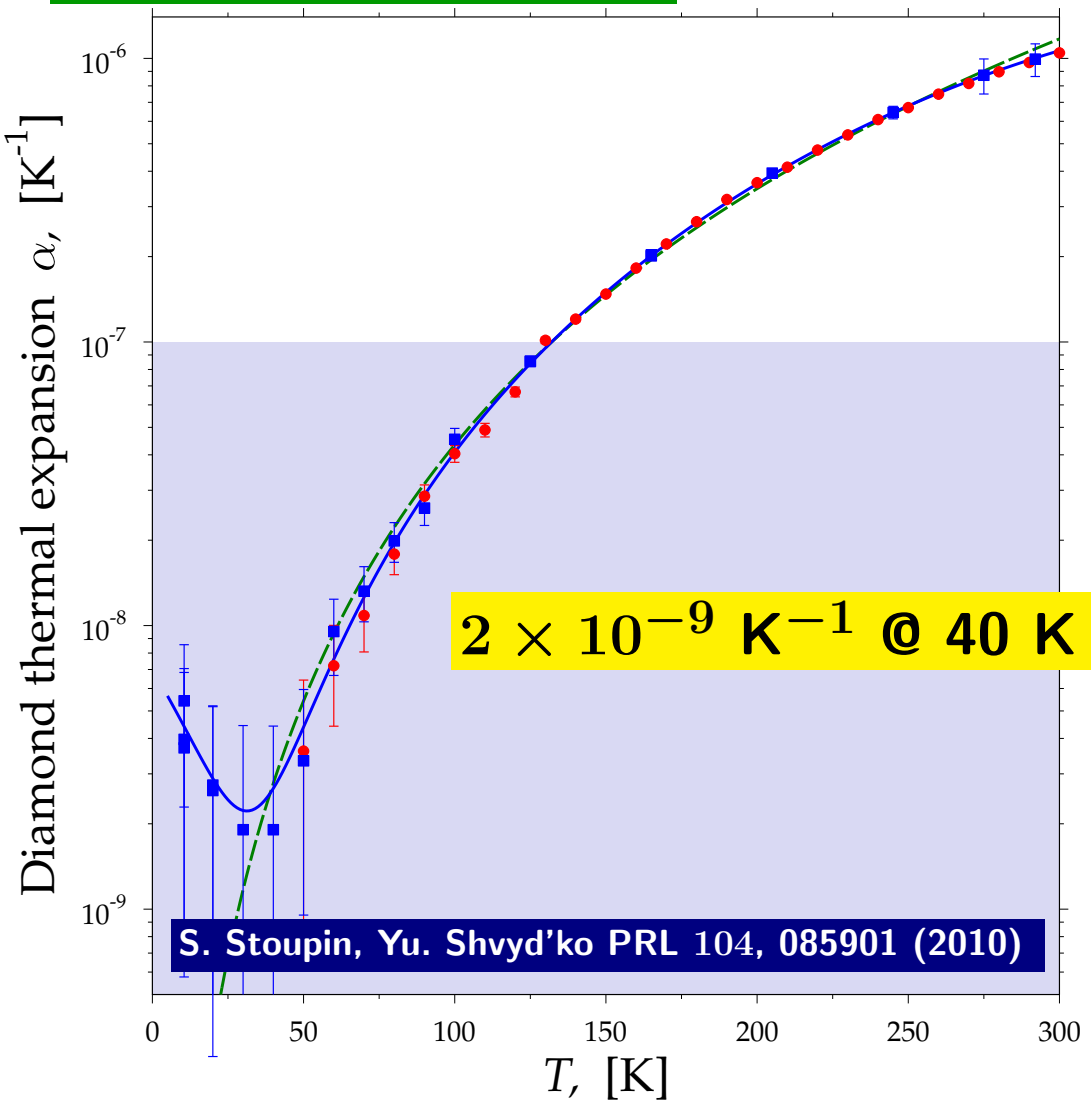

Angular & Spatial Stability

Angular & Spatial Stability

Required angular stability: $\delta\theta \lesssim 10$ **nrad (rms)**
Required spatial stability: $\delta L \lesssim 3$ μ**m (rms)** $\Rightarrow \delta L/L \simeq 3 \times 10^{-8}$ ($L = 100$ **m**)

Angular & Spatial Stability

Required angular stability: $\delta\theta \lesssim 10$ **nrad (rms)**
Required spatial stability: $\delta L \lesssim 3$ μ**m (rms)** $\Rightarrow \delta L/L \simeq 3 \times 10^{-8}$ ($L = 100$ **m**)

Solution: **Null-detection hardware feedback.** **(LIGO prototype)**

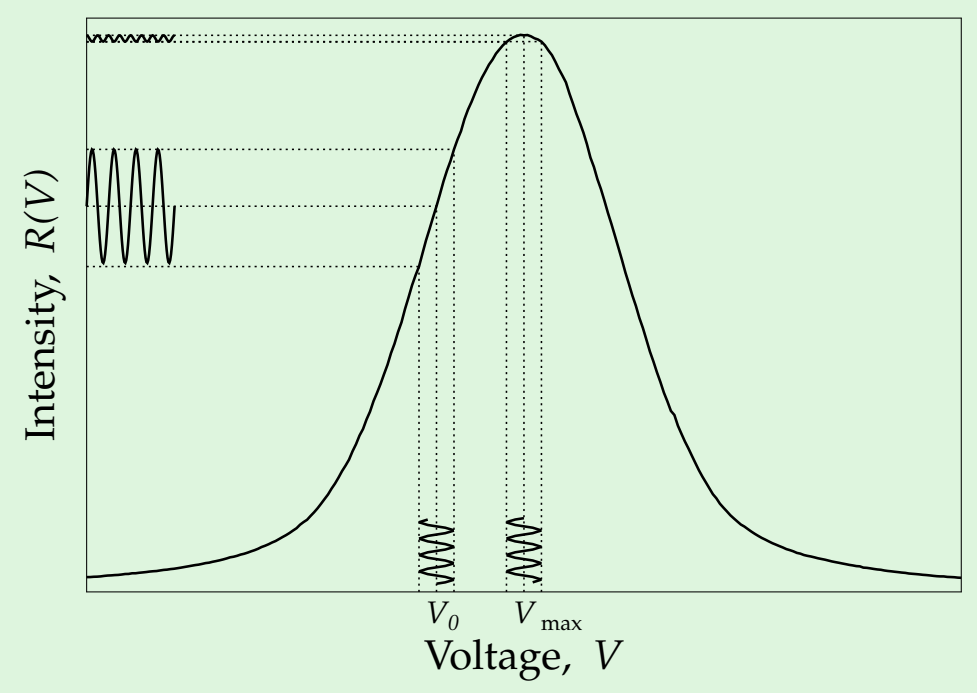

X-ray intensity: **linear response to small angular oscillations is proportional to angular deviation from the maximum of the rocking curve.**

Angular & Spatial Stability

Required angular stability: $\delta\theta \lesssim 10$ **nrad (rms)**
Required spatial stability: $\delta L \lesssim 3$ μ**m (rms)** $\Rightarrow \delta L/L \simeq 3 \times 10^{-8}$ $(L = 100$ **m)**

Solution: **Null-detection hardware feedback.** **(LIGO prototype)**

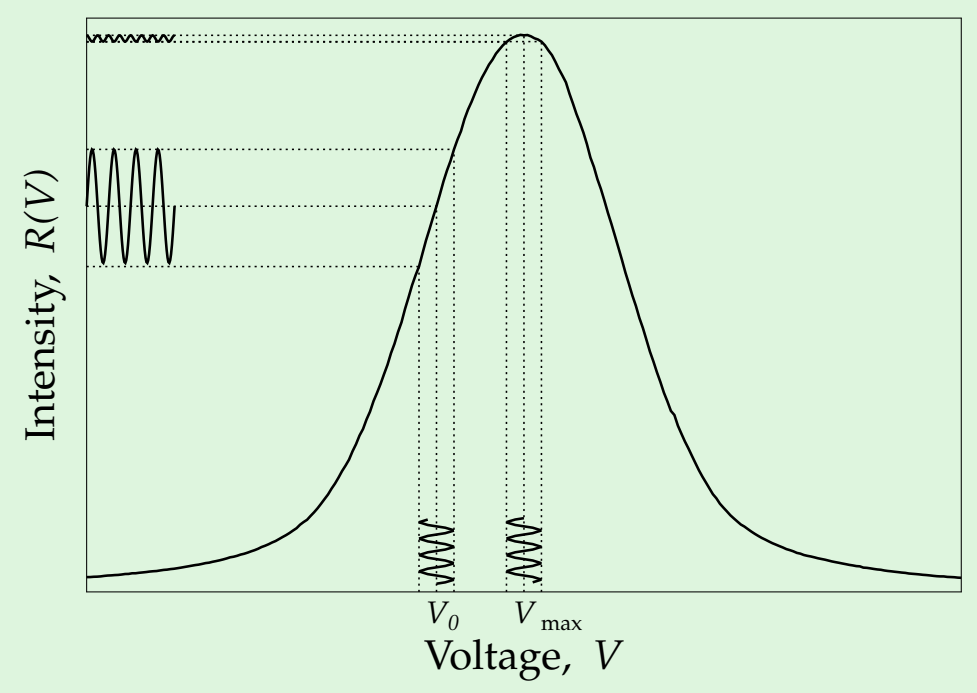

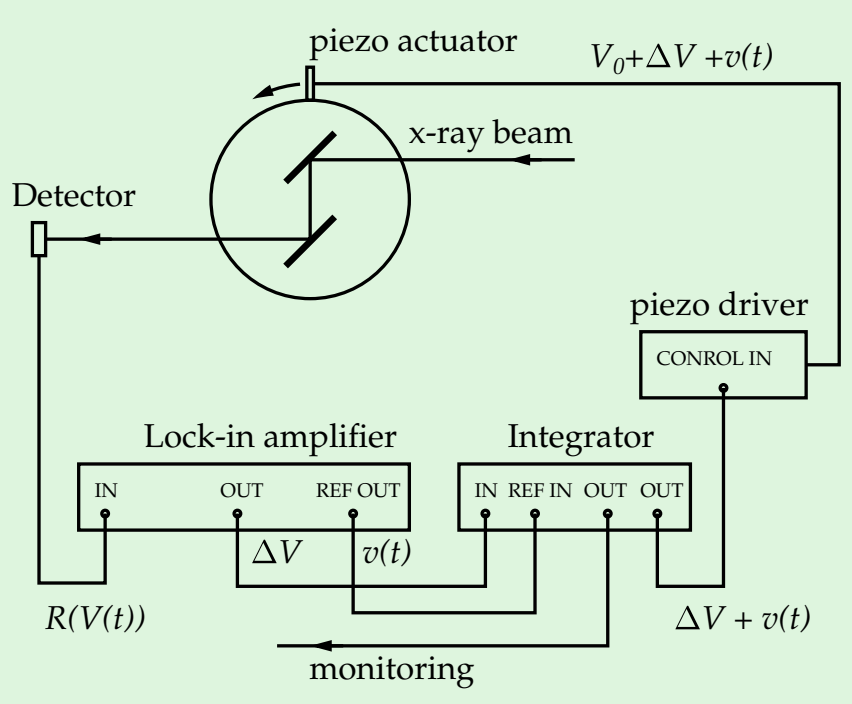

X-ray intensity: **linear response to small angular oscillations is proportional to angular deviation from the maximum of the rocking curve.**

Feedback: **correction signal is extracted using lock-in amplification.**

HERIX Monochromator Stability Region

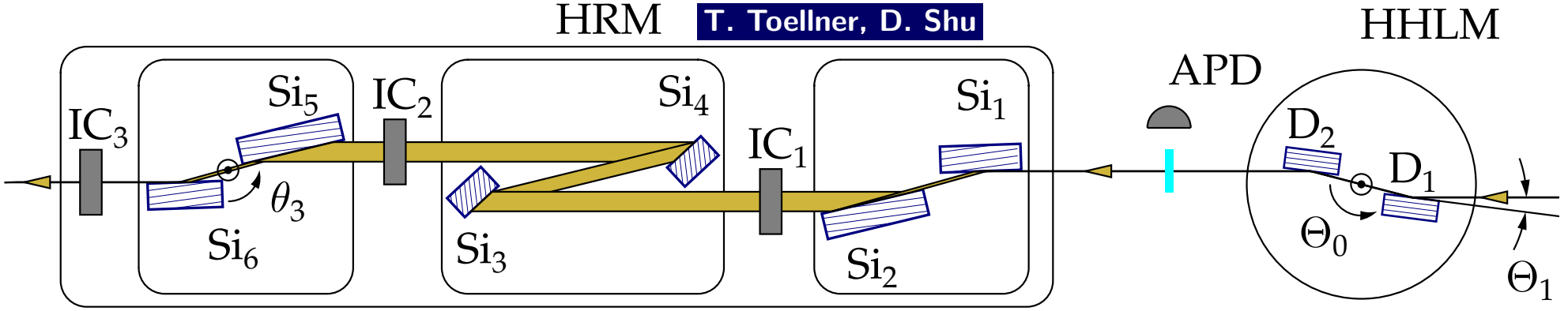

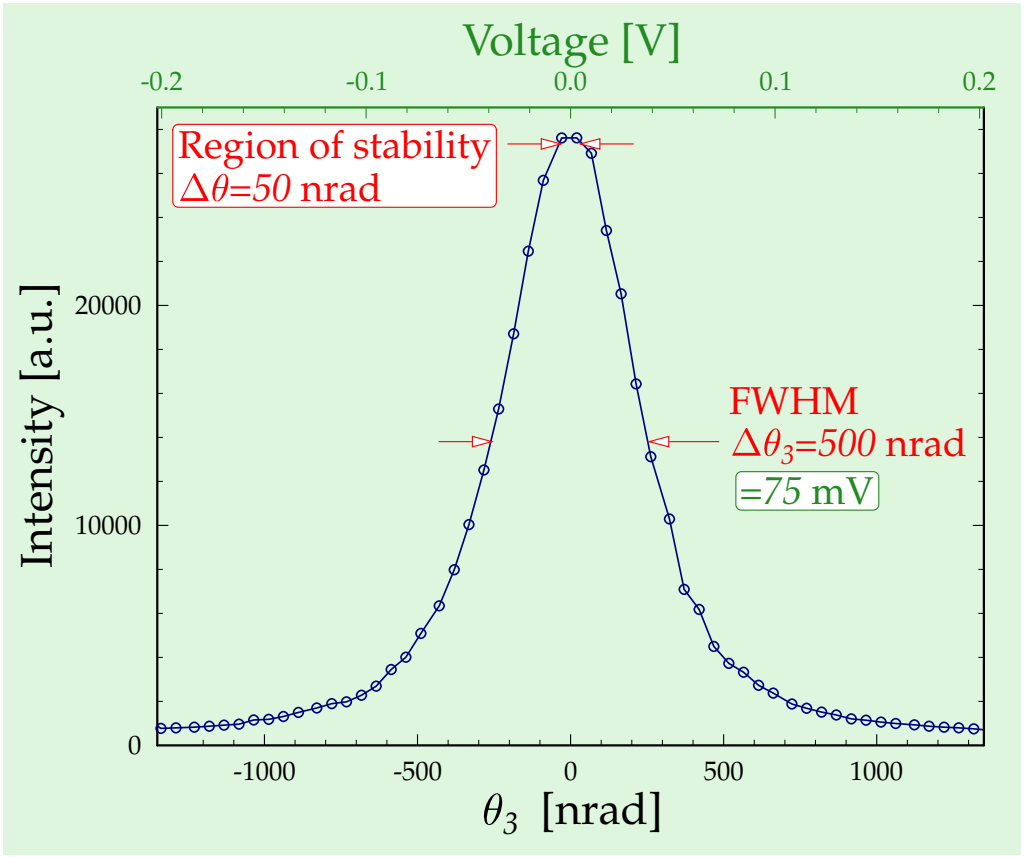

HERIX Monochromator Stabilization

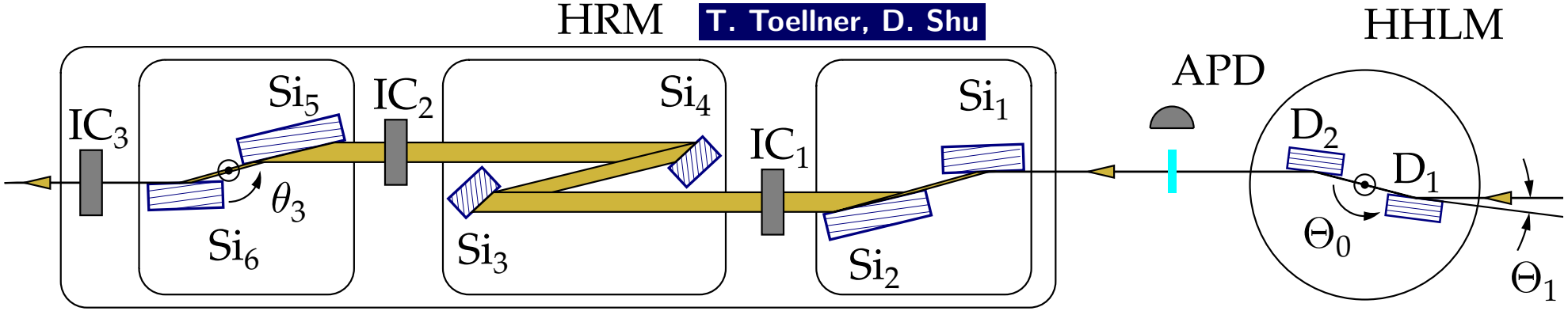

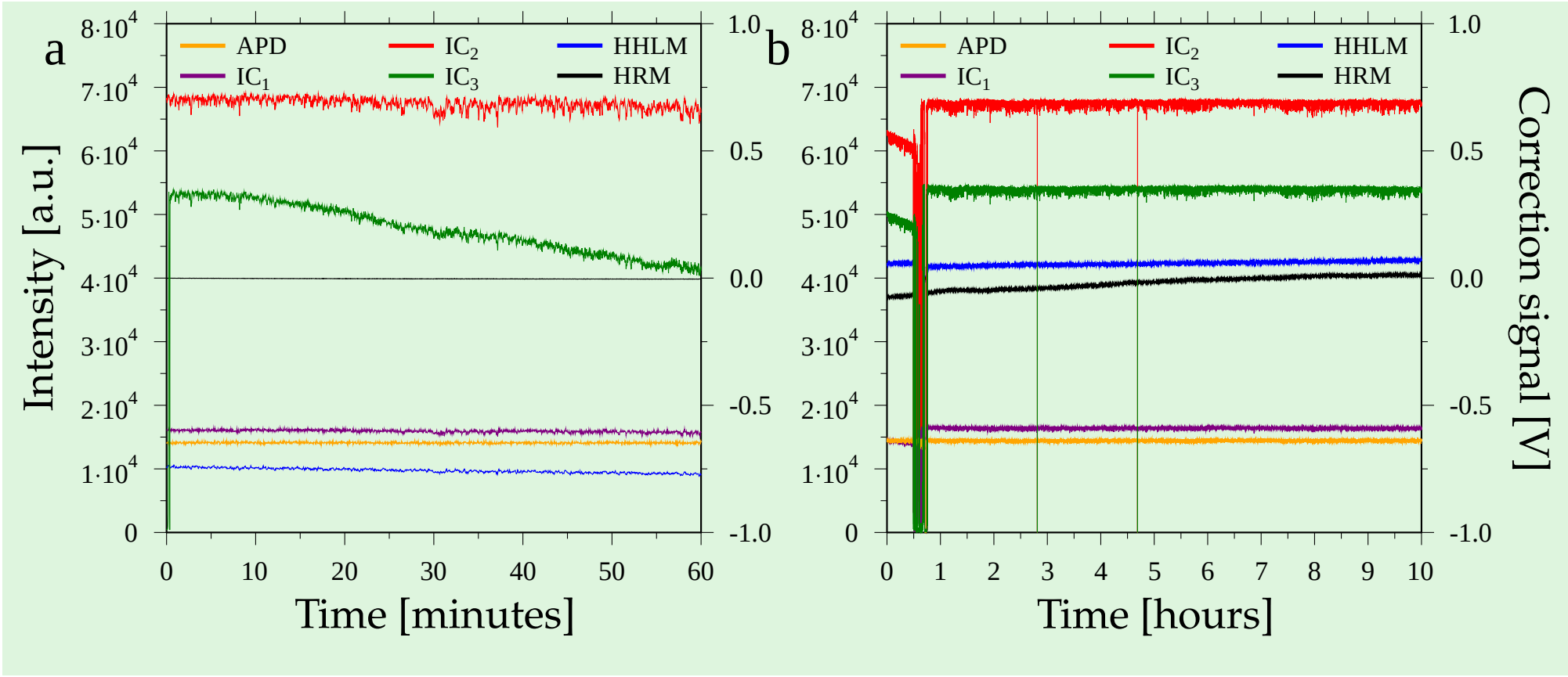

HERIX Monochromator Stabilization

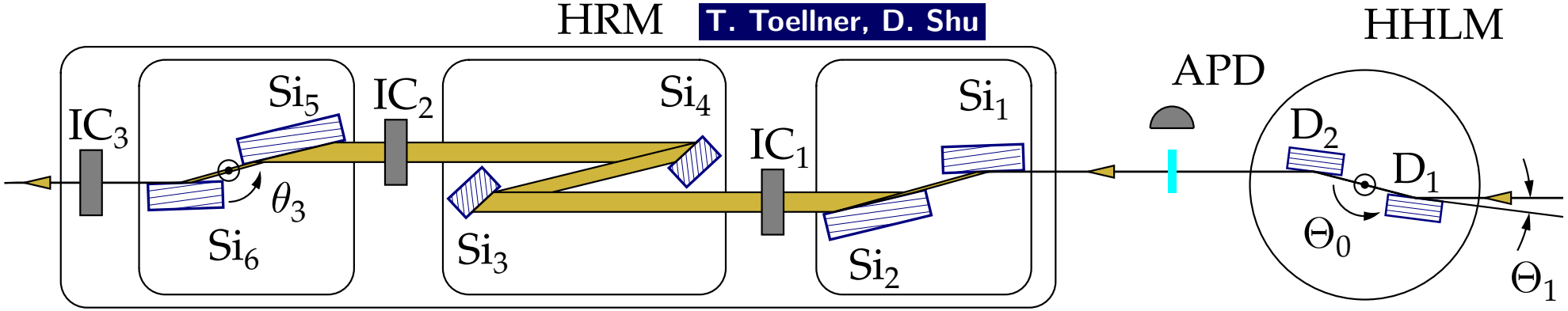

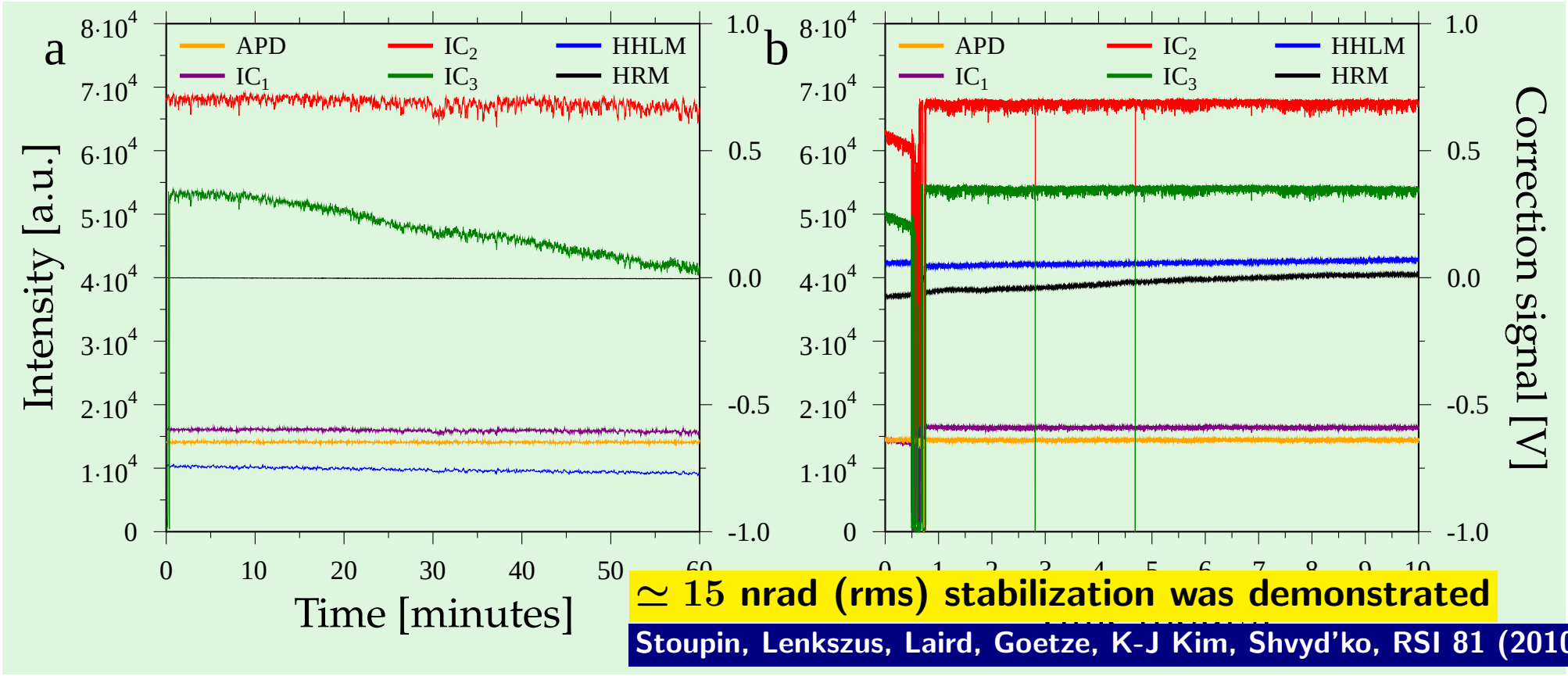

≃ 15 nrad (rms) stabilization was demonstrated

Stoupin, Lenkszus, Laird, Goetze, K-J Kim, Shvyd'ko, RSI 81 (2010) 055108

Resilience of Diamond to Radiation Damage

Resilience of Diamond to Radiation Damage

XFELO generates:

50μJ/pulse @ 12 keV with $\simeq 1$ MHz rep. rate
Footprint: $A = 1.6 \times 10^{-2}$ mm^2 (rms)
Flux density $\simeq 2 \times 10^{18}$ ph/s/mm^2 $\simeq 4$ kW/mm^2

Time to ionize carbon atom with 100% probability: $T \simeq 250$ s Robin Santra

Can this produce irreversible changes in the perfect crystal lattice structure?

Resilience of Diamond to Radiation Damage

XFELO generates:

50μJ/pulse @ 12 keV with $\simeq 1$ MHz rep. rate
Footprint: $A = 1.6 \times 10^{-2}$ mm^2 (rms)
Flux density $\simeq 2 \times 10^{18}$ ph/s/mm^2 $\simeq 4$ kW/mm^2

Time to ionize carbon atom with 100% probability: $T \simeq 250$ s Robin Santra

APS undulators generate:

Flux density $\simeq 5 \times 10^{15}$ ph/s/mm^2 $\simeq 0.15$ kW/mm^2

Time to ionize carbon atom with 100% probability: $T' \simeq 10^5$ s $\simeq 1$ day

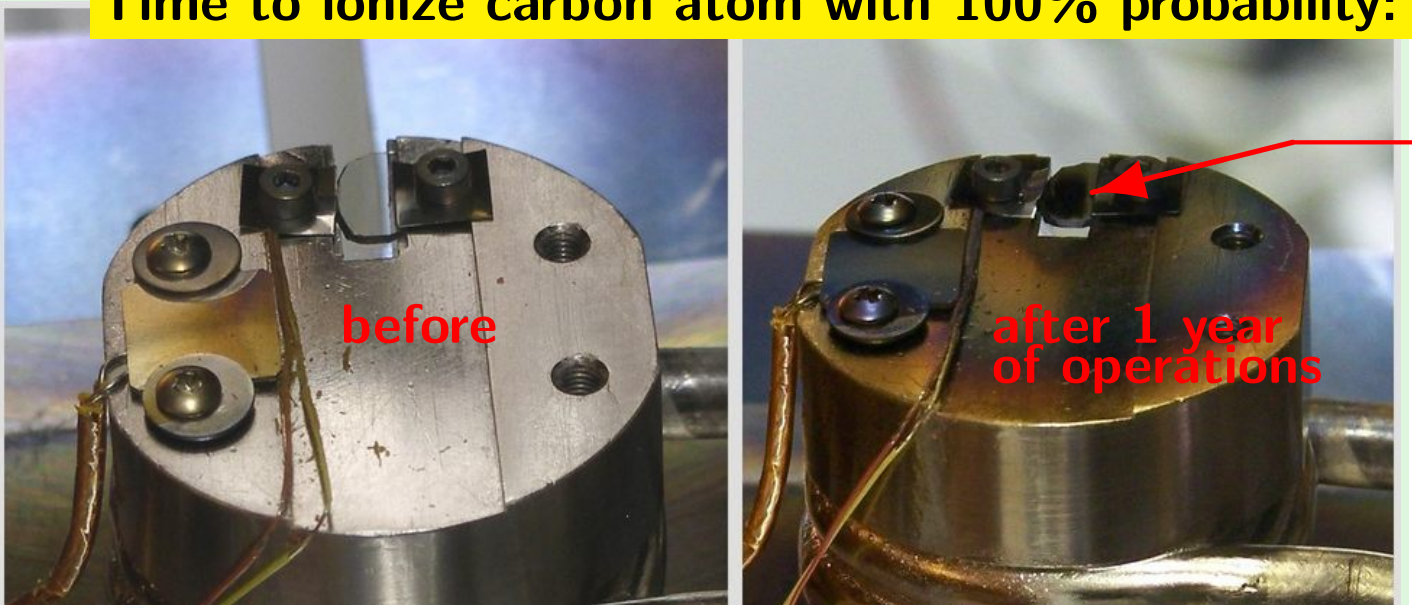

Graphitization of the surface layer of the diamond crystal is observed after several days of operations. Though, no significant degradation in the performance of the high-heat-load monochromator is observed after a year of operations.

Diamond under 3.5 kW/mm^2 load survives

J. Als-Nielsen, A. K. Freund, et al, NIM, B94, 348-350 (1994).

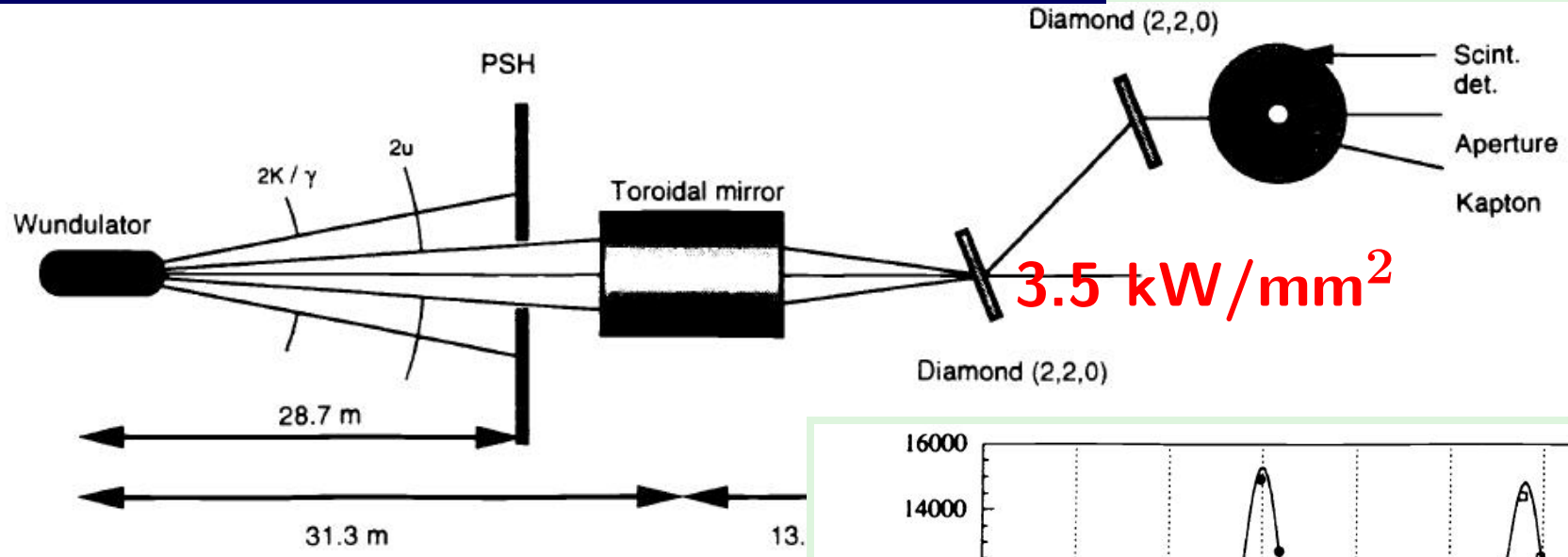

Fig. 2 Schematic diagram of the experimental setup

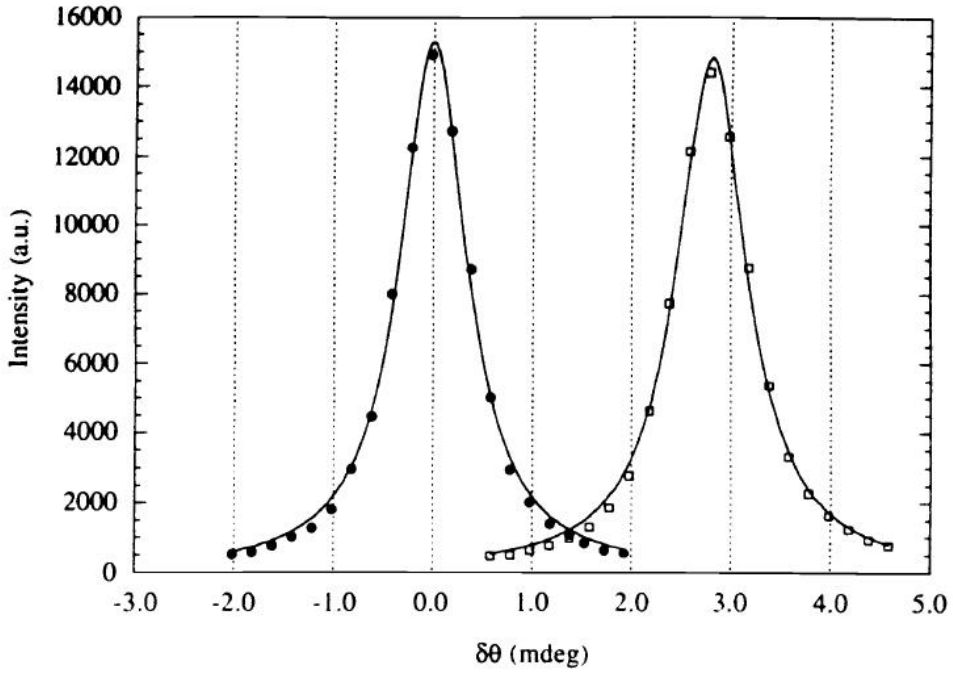

Fig. 3 Rocking curves of the analyzer at low and high power levels. The full lines are least squares fitted Lorentzians.[26]

APS Experiments on Resilience of Diamond Exposed to High-Power-Density X-rays

- 34 ID-E: 4 kW/mm^2 in 0.5x0.5 μm^2
- 35 ID-B: 8 kW/mm^2 in 120x30 μm^2 spot (~XFELO)
- Raman characterization (of surface contamination)
- Double crystal topography at 1BM-B

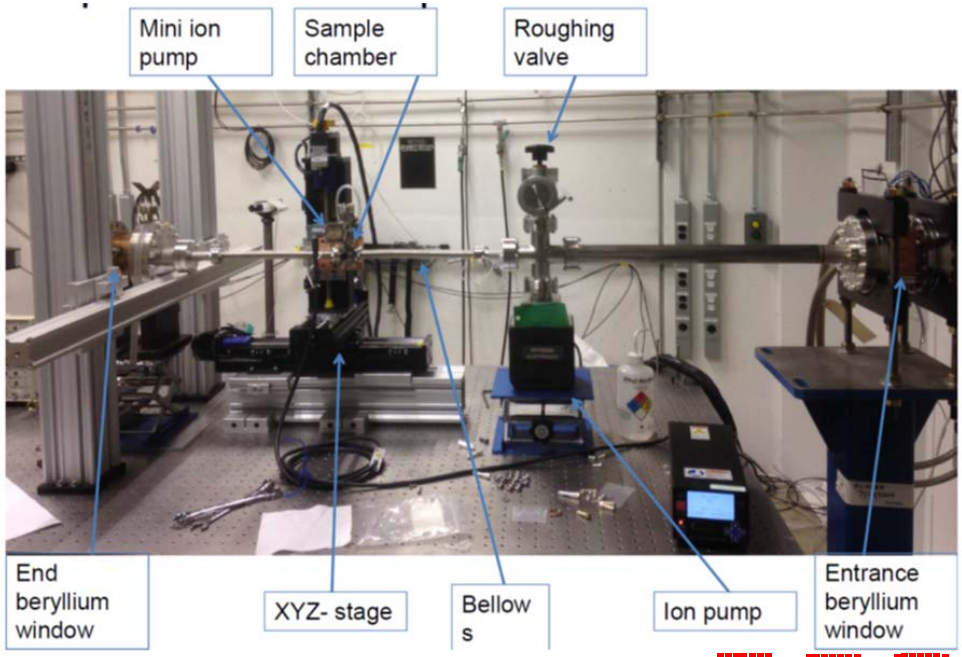

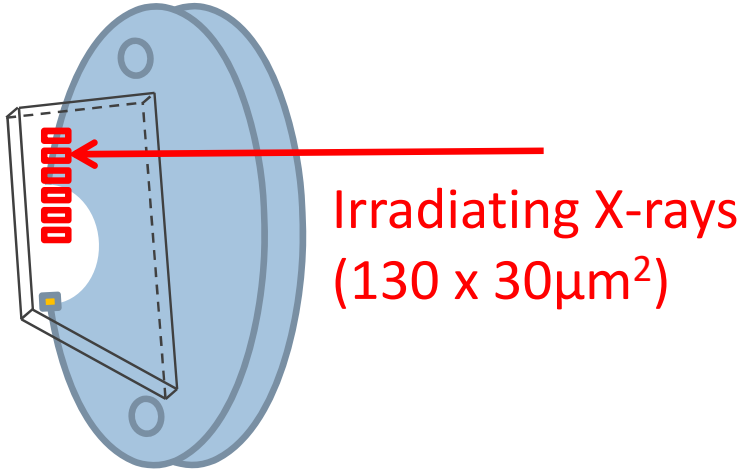

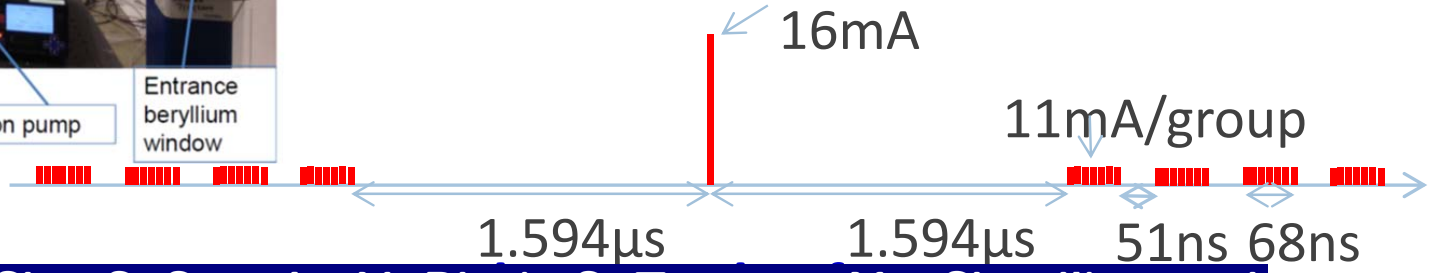

T. Kolodziej, K.-J.Kim, Deming Shu, S. Stoupin, V. Blank, S. Terentev, Yu. Shvyd'ko, et al

No Structural Changes are Observed with Medium Resolution (10^{-6}) X-ray Topography

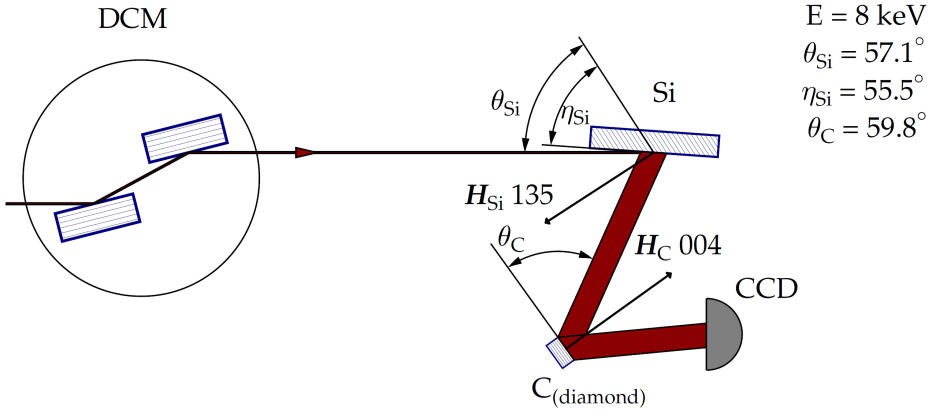

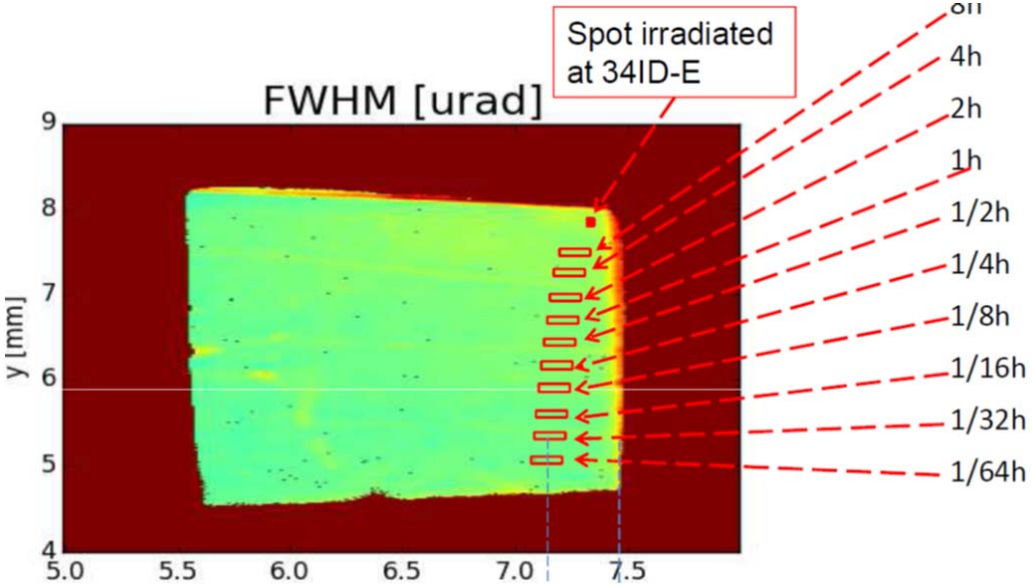

Raman spectra

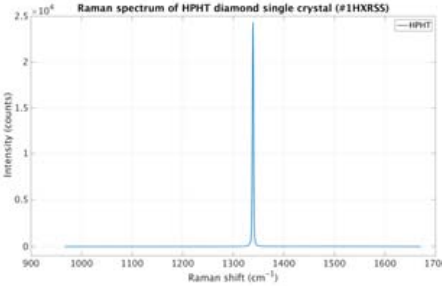

HPHT diamond

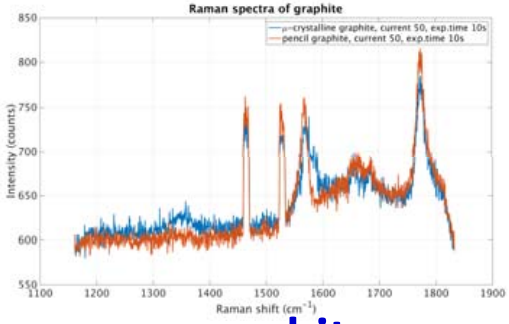

graphite

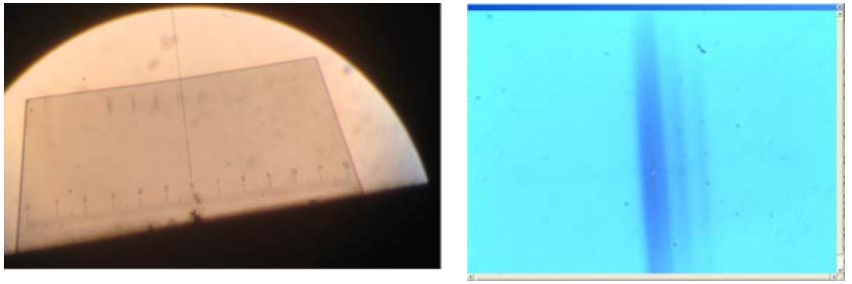

Optical microscope images

Bragg-Reflection Curve Shifts are Observed with High-Resolution (10^{-8}) X-ray Diffraction

Experiment scheme

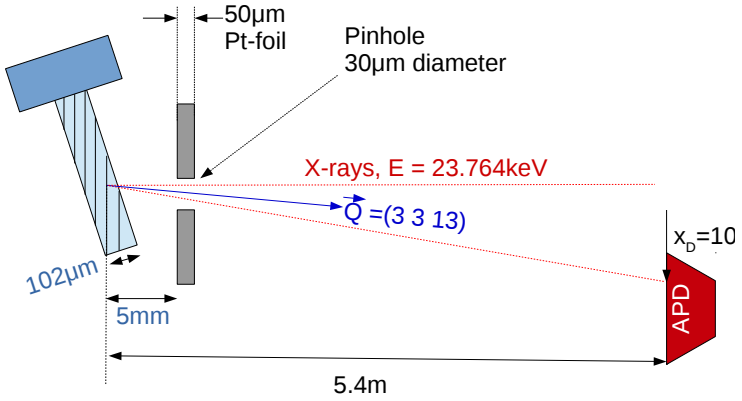

$E = 23.76$ keV, $\Delta E = 1$ meV

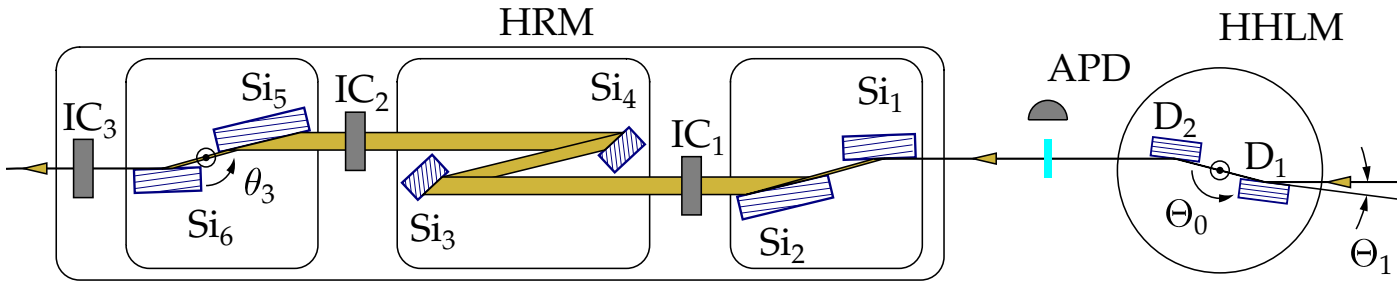

T. Kolodziej, K.-J.Kim, D. Shu, A. Said, V. Blank, S. Terentev, Yu. Shvyd'ko, et al

Bragg-Reflection Curve Shifts are Observed with High-Resolution (10^{-8}) X-ray Diffraction

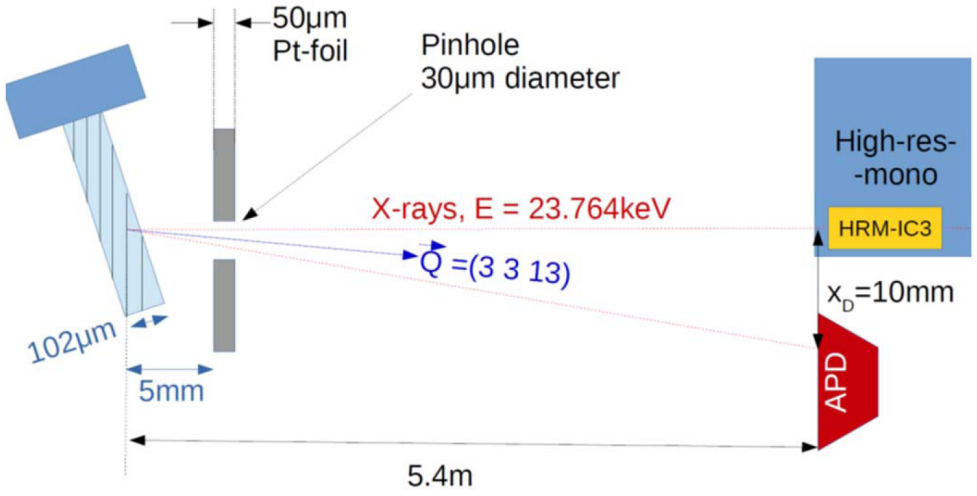

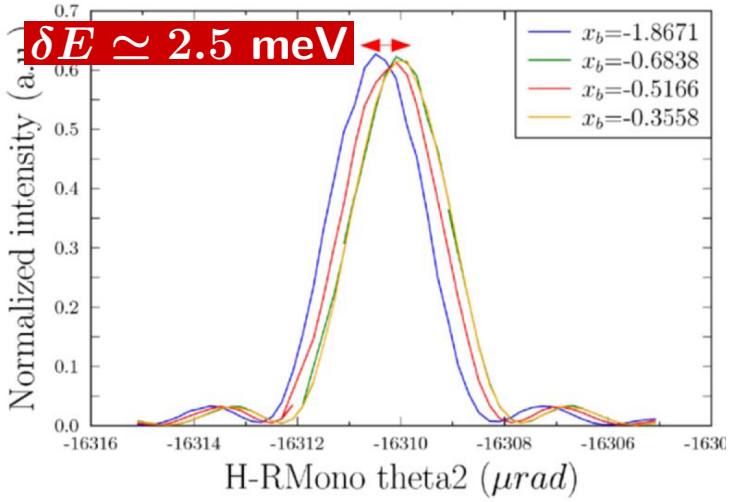

- $\simeq 1$ meV shifts of the Bragg-reflection curves are observed in the irradiated areas.
- Reflectivity and width are not changed!!!
- Presumably, it is a bulk effect of the irradiation (crystal swells).
- Uncritical if the Bragg reflection widths are $\gtrsim 10$ meV, as typical for $E \lesssim 15-17$ keV.
- Could be compensated by the angular correction of the crystal.

T. Kolodziej, K.-J.Kim, D. Shu, A. Said, V. Blank, S. Terentev, Yu. Shvyd'ko, et al

Conclusions and Outlook

Yet no show-stoppers for XFELO cavities were detected:

- **Quality of diamond crystals:** ✓
  theoretical $\simeq 99\%$ reflectivity is achievable.
- **Focusing and collimating optics suitable for XFELO cavities are available.** ✓
- **Heat load problem:** ✓
  simulations indicate that Bragg reflection region variations can be $\lesssim 1$ meV.
- **Angular stability:** ✓
  $\delta\theta \simeq 15$ nrad (rms) can be achieved

(multi-axis stabilization tests are required)

- **Resilience to radiation damage:** ✓ **with an accuracy of $> 10^{-7}$.**

(refined studies are required)

Conclusions and Outlook

Yet no show-stoppers for XFELO cavities were detected:

- **Quality of diamond crystals:** ✓
  theoretical $\simeq 99\%$ reflectivity is achievable.
- **Focusing and collimating optics suitable for XFELO cavities are available.** ✓
- **Heat load problem:** ✓
  simulations indicate that Bragg reflection region variations can be $\lesssim 1$ meV.
- **Angular stability:** ✓
  $\delta\theta \simeq 15$ nrad (rms) can be achieved

(multi-axis stabilization tests are required)

- **Resilience to radiation damage:** ✓ **with an accuracy of $> 10^{-7}$.**

(refined studies are required)

Thank you for your attention

Berman, L. E., Hastings, J., Siddons, D. P., Koike, M., Stojanoff, V. and Hart, M.: 1993, Diamond crystal x-ray optics for high-power-density synchrotron radiation beams, Nucl. Instrum. Methods Phys. Res. A 329, 555–563.

Burns, R. C., Chumakov, A. I., Connell, S. H., Dube, D., Godfried, H. P., Hansen, J. O., Härtwig, J., Hoszowska, J., Masiello, F., Mkhonza, L., Rebak, M., Rommevaux, A., Setshedi, R. and Vaerenbergh, P. V.: 2009, HPHT growth and x-ray characterization of high-quality type IIa diamond, J. Phys.: Condensed Matter 21, 364224(14pp).

Fernandez, P., Graber, T., Lee, W.-K., Mills, D., Rogers, C. and Assoufid, L.: 1997, Test of a high-heat-load double-crystal diamond monochromator at the Advanced Photon Source, Nucl. Instrum. Methods Phys. Res. A 400, 476–483.

Freund, A. K.: 1995, Diamond single crystals: the ultimate monochromator material for high-power x-ray beams, Optical Engineering 34(2), 432–440.

Pal'yanov, Y., Malinovsky, Y., Borzdov, Y. M. and Khokryakov, A. F.: 1990, Use of the "split sphere" apparatus for growing large diamond crystals without the use of a hydraulic press, Doklady Akademii Nauk SSSR 315, 233–237.

Polyakov, S. N., Denisov, V. N., Kuzmin, N. V., Kuznetsov, M. S., Martyushov, S. Y., Nosukhin, S. A., Terentiev, S. A. and Blank, V. D.: 2011, Characteriza-

tion of top-quality type iia synthetic diamonds for new x-ray optics, Diamond and Related Materials 20(5-6), 726–728.

Sellschop, J. P. F., Connell, S. H., Nilen, R. W. N., Detlefs, C., Freund, A. K., Hoszowska, J., Hustache, R., Burns, R. C., Rebak, M., Hansen, J. O., Welch, D. L. and Hall, C.: 2000, Synchrotron x-ray applications of synthetic diamonds, New Diamond and Frontier Carbon Technology 10, 253–258.

Sumiya, H. and Satoh, S.: 1996, High-pressure synthesis of high-purity diamond crystal, Diamond and Related Materials 5, 1359–1365.

Sumiya, H., Toda, N. and Satoh, S.: 2000, High-quality large diamond crystals, New Diamond and Frontier Carbon Technol. 10, 233–251.

Yabashi, M., Goto, S., Shimizu, Y., Tamasaku, K., Yamazaki, H., Yoda, Y., Suzuki, M., Ohishi, Y., Yamamoto, M. and Ishikawa, T.: 2007, Diamond double-crystal monochromator for spring-8 undulator beamlines, AIP Conf. Proc. 879, 922–925.

Zhong, Y., Macrander, A. T., Krasnicki, S., Chu, Y. S., Maj, J., Assoufid, L. and Qian, J.: 2007, Rocking curve FWHM maps of a chemically etched (001) oriented HPHT type Ib diamond crystal plate, J. Phys. D: Appl. Phys. 40, 5301–5305.

Wavefront upon Bragg Reflection C(004)

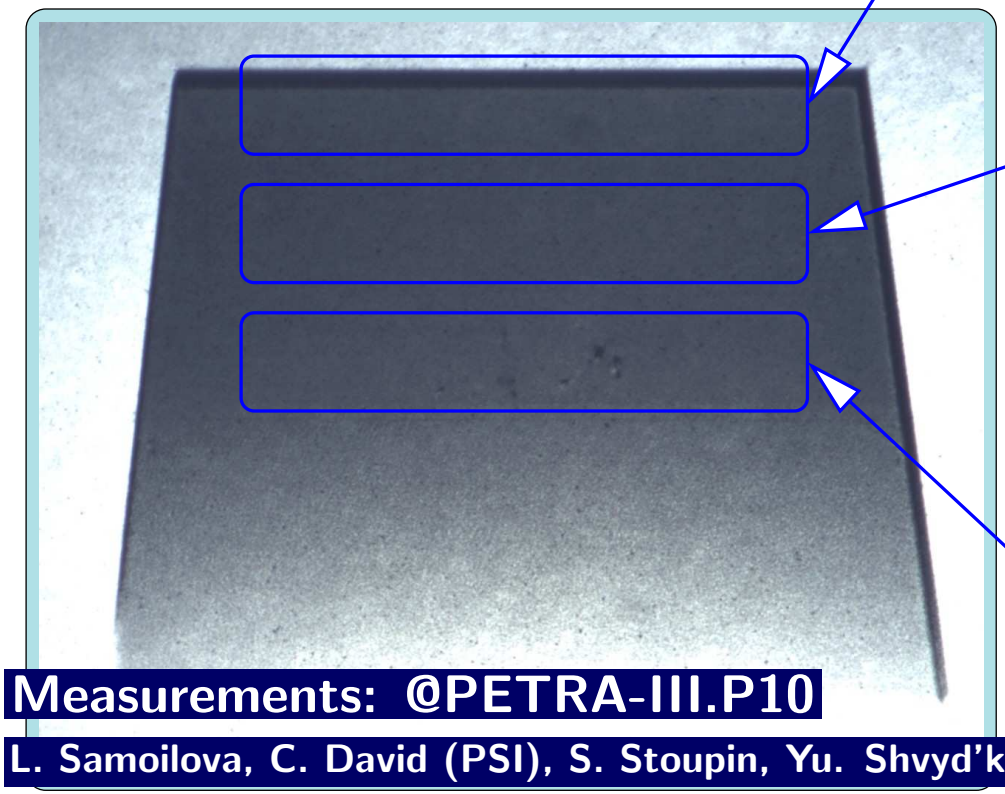

Moire fringes with x-ray Talbot interferometer

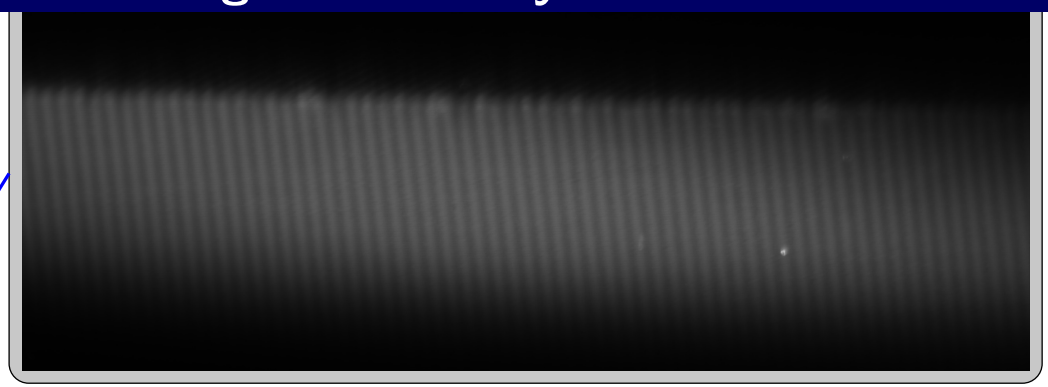

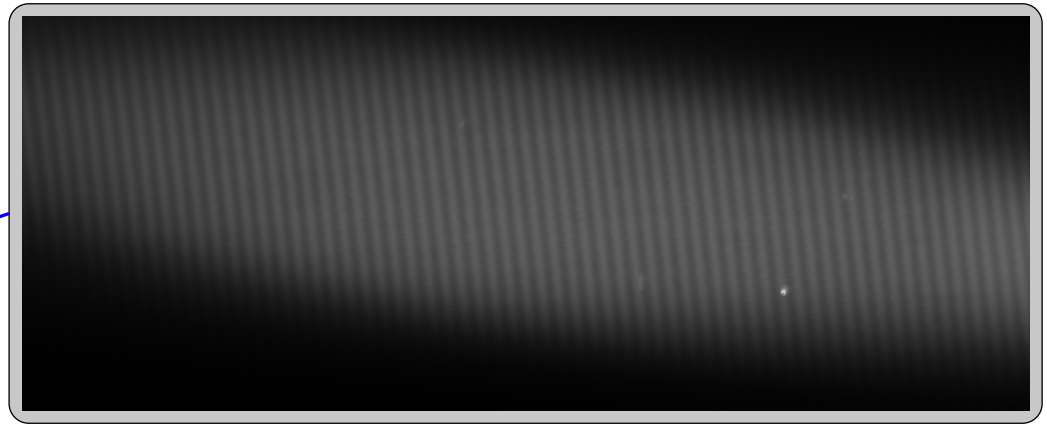

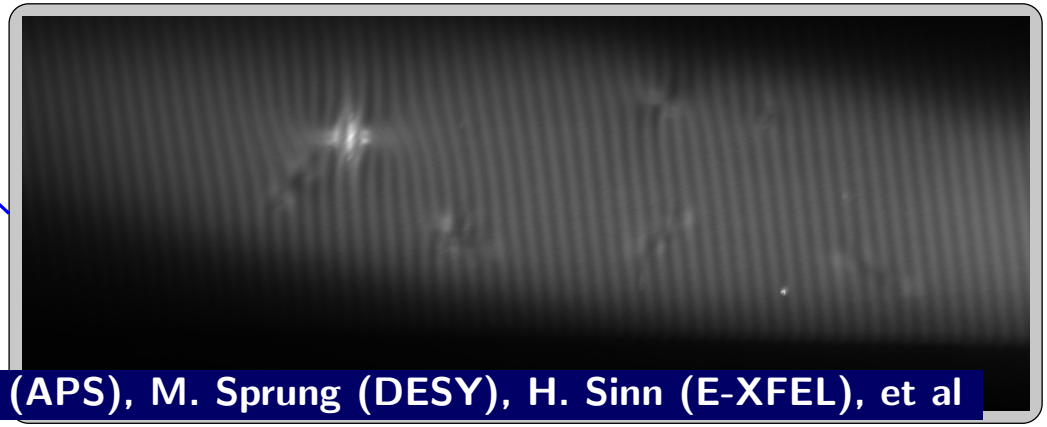

Measurements: @PETRA-III.P10

L. Samoilova, C. David (PSI), S. Stoupin, Yu. Shvyd'ko (APS), M. Sprung (DESY), H. Sinn (E-XFEL), et al

Wavefront upon Bragg Reflection C(004)

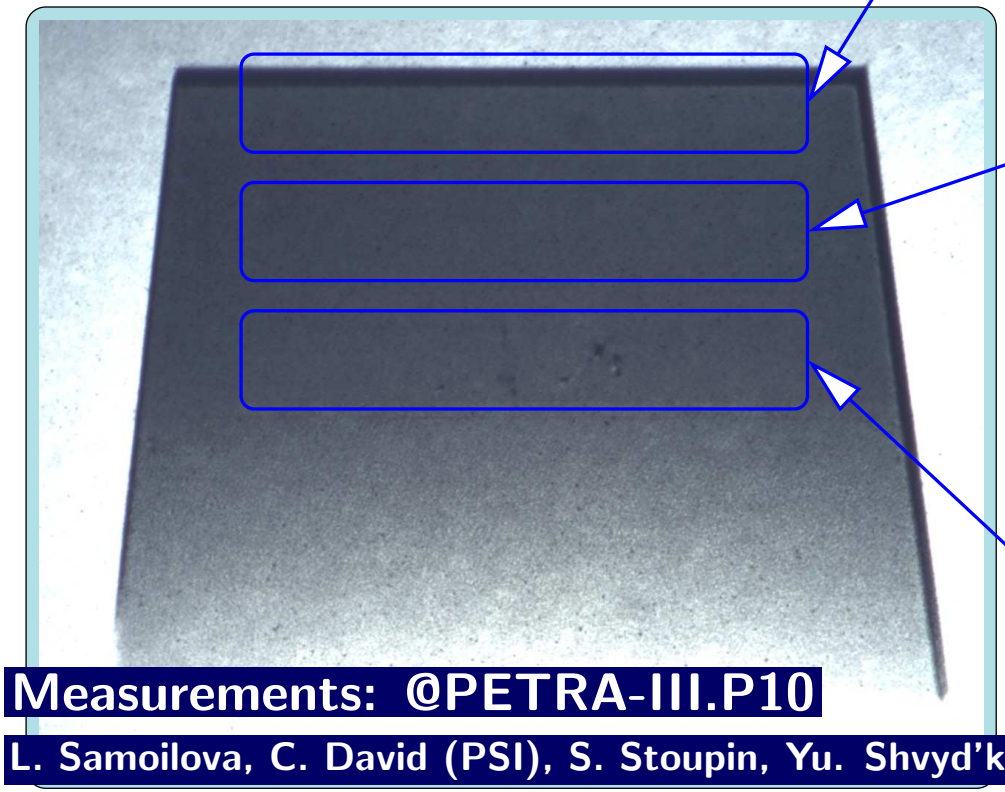

Moire fringes with x-ray Talbot interferometer

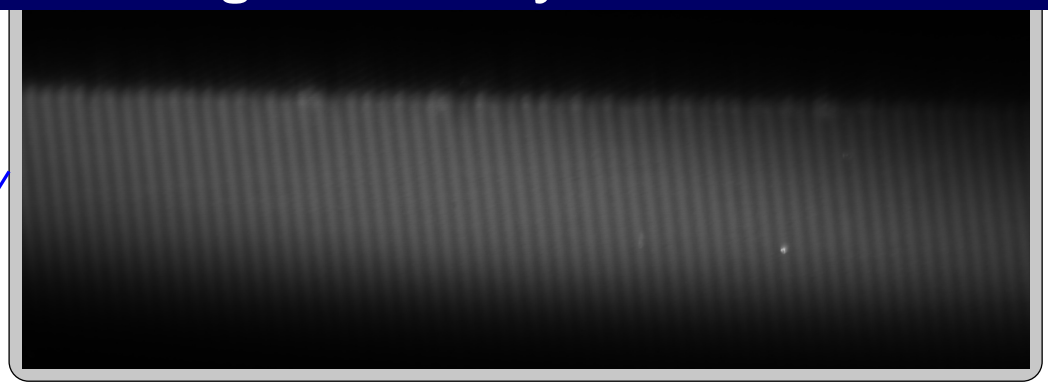

Wavefront distortions $\lesssim 1$ μrad.

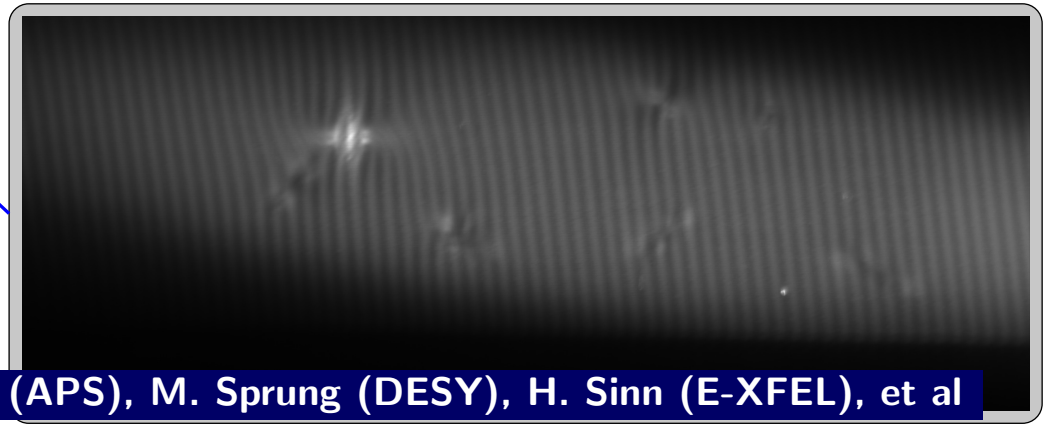

Measurements: @PETRA-III.P10

L. Samoilova, C. David (PSI), S. Stoupin, Yu. Shvyd'ko (APS), M. Sprung (DESY), H. Sinn (E-XFEL), et al